Point-to-point reply #2 to Reviewer #2 comments by Leupold et al.

Dear Luc Beaufort,

We are grateful for the feedback provided by the anonymous reviewer and for your decision letter. Below, we address all items raised by the reviewer in detail. We added the wavelet spectrums of all coral records to the supplementary material as suggested by the reviewer and explained why we still prefer showing the wavelet coherence plots in the main document of the manuscript. Furthermore, the manuscript was checked for grammar issues and unclear sentences and for consistent use of the tense.
In the following, we will repeat the reviewer's statement (in normal font) and our reply to it (in italic font). Numbers in brackets at the beginning of our comments indicate line numbers of the revised version of the manuscript with highlighted changes.

Yours sincerely, Maike Leupold

Editor Decision: Publish subject to minor revisions (review by editor) (12 Oct 2020) by Luc Beaufort
Comments to the Author:
Dear Maike Leupold and co-ahthors,
Your manuscript has been reviewed a second time by the most critical reviewer of the original submission. He/she is now satisfied with the revisions you made to the original manuscript. Some points need to be corrected and I suggest that you do so. I will check your corrections myself. Also, the reviewer is quite critical of the quality of the syntax, and asks you to have the article corrected by someone qualified. I would appreciate it if you would follow his/her advice.
Yours sincerely, Luc Beaufort

Report Anonymous Referee #2:
This revised paper is improved and many details that were unclear in the previous revision are now improved. The detailed analysis of ENSO events with two different reference data sources highlights the discrepancies that any reconstruction will have but still supports the results of the current study. The discussion section begins more like a conclusion section. The discussion should be a comparison to other work, discussion of the strength and weakness of your results, and other interpretations, and implications of the study.

We agree with the reviewer that the discussion section began like a conclusion. We revised the entire section.

This paper still has many grammar issues and unclear sentences. I suggest the authors get help to address these issues. I do not take the time to note all these issues in my detailed edits since there are many and this is a second review. I tried to focus on the science. But this paper needs to have the grammar addressed before publication. I use the free website Grammarly.com often and recommend my students use it as well.

The manuscript was checked for grammar and syntax issues.

Science items to address:
The wavelet coherence plots are interesting, but the authors do not take chronology error into account. Assuming the Wilson Nino reconstruction does not have chronology errors, if you shift the coral chronologies within the U-Th dating uncertainties, do the wavelet coherence plots

change or find better coherence? With U-Th errors or ±2-3 years, 2d, you could shift by 6 years to see if the results are better or worse. These plots as they as presented are not showing the level of coherence I would expect if there was a strong ENSO signal in these records. I would like to see the Wavelet spectrums of the coral records to see what the ENSO periodicities look like, I would buy that more than the coherence with two reconstructions that both have chronology errors that could greatly impact these results, see Comboul 2014, doi:10.5194/cp-10-825-2014.

This comment is somewhat contradictory to an earlier comment from anonymous reviewer 2 (see our previous response letter):

„Spectral analysis is suggestive of periodicities similar to ENSO but is NOT conclusive evidence, see Hochman et al. 2019 (doi: 10.1175/jamc-d-18-0331.1) and Liu et al 2007 (doi: 10.1175/2007jtecho511.1). A large anomaly with the width of 2-7 years can be manifested as a significant 2-7 year periodicity in a spectrum leading to the misinterpretation of ENSO periodicity (try for yourself, do a FFT spectrum and wavelet spectrum of the volcanic explosivity index and compare).“

Because of this comment, we decided to include the wavelet coherency plots in the main text of our revised manuscript.

'Normal' Wavelet spectrums are – just like other methods of spectral analysis – suggestive of periodicities but NOT conclusive evidence, although they do show interannual variability in time/frequency space.

We therefore used wavelet coherence analysis to detect common (coherent) time-localized oscillations in the Wilson Nino Index and the Chagos coral Sr/Ca records. We view one time series (the Wilson Nino Index which is based on a multiproxy reconstruction) as influencing the other (Chagos SST, inferred from coral Sr/Ca). This means we can use the phase of the wavelet cross-spectrum to identify the relative lag between the two time series. This lag is mentioned in the manuscript text, and we suggest that it reflects the age uncertainty of the sub-fossil Chagos corals. [Note that Indian Ocean warming (cooling) appears during peak ENSO warming (cooling) in December-February and decays in the following boreal spring].

Comboul et al. (2014) assess time-variant age model errors that may result from the miscounting of annual density bands/seasonal coral Sr/Ca cycles and how these could influence the spectral characteristics of proxy time series. (Wavelet coherency analysis is not discussed in this paper). The authors show that these age model uncertainties may reduce the coherency between two time series (but they do not inflate it). While we cannot rule this out, we find significant coherencies between the Wilson Nino Index and our coral Sr/Ca records.

We show the raw Sr/Ca data together with the X-ray images in the supplements so that our age models can be assessed.

Furthermore, the GIM core (and two other modern replication cores from Chagos) which derive from absolutely dated modern corals capture ENSO variability in the central Indian Ocean (e.g. Pfeiffer et al., 2017, https://doi.org/10.1038/s41598-017-14352-6; Pfeiffer et al., 2009, https://doi.org/10.1007/s00531-008-0326-z; Pfeiffer et al., 2006, https://doi.org/10.1130/g23162a.1). In fact, the corals show a significant linear correlation with Nino3.4 SST and the Palmyra coral $\delta^{18}O$ record published by Kim Cobb (Pfeiffer et al., 2009, https://doi.org/10.1007/s00531-008-0326-z).

However, to address this scientific item, we added 'normal' wavelet power spectra of all coral records analyzed in our study to the supplementary material (Figure S7). All coral time series show significant interannual variability in the ENSO frequency band.

Specific items to address:

What the tense in your paragraph and sections and make sure the tense is consistent. There are still many grammar errors and typos in this paper that need to be corrected before publication.

Line 22 By one sample and two samples, do you mean coral or one measurement for this entire interval. Just say one coral and two corals.

(l. 22) We mean coral sample(s) and revised the sentence.

Figure 1 What are numbers 640, 645, 650, 655 for on the right side of the map? Put the latitude and longitude degrees outside the box since the inset is covering part of the or move latitude to the right side of the map. It would be helpful if you map the mean SST of SST anomalies on this map to show the difference note in section 2.3.

(l. 637) The numbers are the line numbers of the document. This probably happened during conversion from Word file to PDF file. We revised Figure 1. Latitudes now appear on the right side of the map. We do not display map mean SST on this map, because it is the seasonal amplitude that makes the difference between both settings and not the mean SST (see our reply to the reviewer's comment "line 113-114" in this document).

Figure 2 The "Red" box for La Nina looks purple to me.

(l. 643) It is the same color as for the box for El Nino. It probably appears different due to the surrounding color of the SST map. Zooming into the boxes confirms that they are actually of the same color.

Figure 3 The blue line looks black to me.

(l. 653) It is dark blue. We added this detail to the subtitle.

Line 38 and 42 and elsewhere Comma is not needed after central "central tropical Indian Ocean".

(l. 41 + 43) Revised.

Line 44 The last phase of the sentence is confusing "…as these are phased-locked to the seasonal cycle and vary with the season" What does "these" refer to? The coral Sr/Ca, the ocean, climate phenomena, or something else. Perhaps clarify what "its" is in the same sentence. Revise to make the meaning clearer.

(l. 44) In this sentence, "these" refers to climate phenomena. We revised this sentence.

Line 46 Explain what you mean by "ENSO is centered". Is this spatially centered? I think you mean "where ENSO occurs". Same for Line 49. The central part of the tropical Pacific Ocean is not where ENSO occurs, ENSO occurs across the tropical Pacific Ocean — East, Central, and West. The central Pacific has the weakest climate response compared to the east and west Pacific. Additionally, there are different favors of ENSO, a central and eastern ENSO as well as a coastal. Therefore, using "centered" is confusing.

(l. 48) We meant "centered" in terms of "mainly affecting". We revised it.

Line 46 Revise "Strong events associated with ENSO have occurred more frequently since the early 1980s relative…"

(l. 48) Revised.

Line 48 and elsewhere - Do not use a "/" to replace the word "and". This is a non-standard replacement, reserve "/" to mean "divide by" or to indicate a ratio like "Sr/Ca". This is an informal usage.

We exchanged every "/" used between "El Niño" and "La Niña" by an "and".

Line 50 Use the adjective form "…oceanic-atmospheric parameters of the Indian Ocean…" Revise the "which" to a "that". The same sentence, use the same tense for the verbs.

(l. 52) Revised.

Line 52-53 Another confusing sentence, what is demonstrating? Revise sentence, a conjunction is needed. "Strong El Niño/La Niña events influence the tropical Indian Ocean thus establishing a SST-ENSO teleconnection between the Pacific and the Indian Ocean." How you do know the teleconnection is "stationary" and for what time interval? Is this a question you can answer with your study or if others have shown this then say "previous studies have established a stationary SST-ENSO teleconnection…".

(l. 54-56) We revised this sentence. We quoted studies stating that the teleconnection was stationary. We consider it to be clear and in agreement with the overall citation style of this manuscript that the references provided in brackets at the end of the sentence refer to the sentence's statement. Therefore, we do not see any reason to revise the sentence with respect to this point.

Line 49 "While" is the incorrect word, you do not mean "at the same time as. If you mean to highlight contrasting relationship use "whereas".

(l. 57) We exchanged "while" by "whereas".

Line 64 Add for clarification the time interval you are referring to for "Indian Ocean warming". Do you mean for the Little Ice Age or just the 20th century?

(l. 67) We meant warming during the 20^{th} century and revised the sentence.

Line 64 Revise "We develop coral Sr/Ca records… to reconstruct past SST variability."

(l. 67) Revised.

Line 99 Revise this confusing incomplete sentence.

(l. 100-101) Revised.

Line 108 What corals are you referring to? The previous sentence refers to two studies. Perhaps you mean "Those corals reconstructions revealed a few strong IOD events…" After reading the following sentence, perhaps you are referring to your own reconstruction that has not been presented yet.

(l. 108) We refer to corals of the studies by Abram et al. And we are not referring to our own reconstructions here. We revised the sentence.

Line 109-112 "However, neither in 1675 nor in 1961 a positive anomaly can be found in our coral SST records." This is a result and the following sentences are how you intend to interpret your results, it does not belong in the introduction, but in the methods or results. Additionally, this sentence is not properly written and thus confusing.

(l. 109-111) Revised.

Line 113-114 How is "28.1±0.9°C for the open ocean and reef and 28.5±0.6°" different from each other? Did you do a statistical test of the mean difference? What is ±0.9ºC? the standard deviation of the mean or standard error of the mean? This is a poorly constructed sentence and all abbreviations should be defined at first use. Revise "Analysis of SST determined from the Advanced Very High-Resolution Radiometer (AVHRR) satellite SST product (Casey et al., 2010) for the varying

grid areas in Chagos (open ocean (give area in degrees) and lagoon (give area in degrees) reveals differences in SST means and seasonality at Chagos depending on the reef setting.
This analysis finds 28.1±0.9°C for the open ocean and reef and 28.5±0.6°C for the lagoon setting averaged over the interval from 1997–2012 (Fig. 3). Not sure what Leupold et al., 2019 is a reference for from the sentence construction. If this figure and analysis is from the study Leupold et al., 2019, this should be made clearer and referenced in Figure 3.

(l. 116-118) We actually wanted to state that the main difference between both settings is rather SST variability than the mean SST and corrected this. We also revised the sentence as suggested by the reviewer.

Line 119-120 Revise for improper use of /, use a hyphen. "such as El Niño in 1997-1998 or La Niña in 2010-2011".

We revised the use of "/" as suggested by the reviewer with one exception: we did not change e.g. 1877/78 to 1877-1878 and similar cases (i.e. kept 1997/98), because in this case "/" is part of a name (e.g. the El Niño event 1997/98) and does not refer to a time period as in e.g. "Little Ice Age (1836-1867)".

Line 119-120 What do you mean by "Both anomaly records are not significantly different (t-value = 0.34; p-value = 0.37)"? Is this a statistical test for the means, variance, or something else? You can also look at correlation to describe co-variance, which is more interesting for an SSTA time series looking at ENSO than if the means and or variance are the same or different.

(l. 124) Yes, it is a common statistical test for the means; it is a t-test. Both values (t- and p-value) are the characteristic parameters for a t-test.

Line 121 The reader does not know anything your coals or about the location your corals yet in the text, revise the text as needed, and refer to Fig. 1 where you have the coral locations.

(l. 124) We do not agree with the reviewer. The entire Section 2 deals with the study site and the location (Chagos) and its climate are sufficiently introduced in Sections 2.1 and 2.2. The fact that this study investigates SST recorded by corals is explicitly mentioned at the end of Section 1. The sentence in Line 121 concludes on the information provided in the very same paragraph and does not need any further clarification.

Line 125 Revise "We therefore use various ENSO indices for comparison with our coral data…"

(l. 129) Revised.

Line 128-129 "TexMex" is not the correct geographical term, use "Texas-Mexico". Define USA abbreviation at first use. Revise "and other locations in the Tropics". Revise "The annually-resolved El Niño Index Niño3.4…reconstructs past El Niño and La Niña events back to 1607." Why is Niño3.4 in italics in this usage? Do not use italics to make it appear different, give it a name different from Niño3.4, which is a defined index used by climatologists to determine ENSO, see https://climatedataguide.ucar.edu/climate-data/nino-sst-indices-nino-12-3-34-4-oni-and-tni. This is not what you mean. Wilson reconstructed the Nino3.4 index in their study but it is not the Nino3.4 index. Refer to it as Wilson Nino3.4 or reconstructed Nino3.4 to make it clear you are referring to the reconstruction and not the average of instrumental SST for 5N-5S, 170W-120W. Even better revision to this sentence "The study of Wilson et al. (2010) reconstructs an annually-resolved Niño3.4 index …of past El Niño and La Niña events back to 1607 beyond the instrumental era, which we will refer to as the "Wilson Niño Index."

(l. 130-133) We revised this sentence.

Line 129-130 Delete “We use the Wilson Niño Index for comparison with our coral SST records performing Wavelet Coherence Analysis in the time domain (see section 4.4).” This does not need to be stated here but in your results.

(l. 133) We will not delete this sentence, because it explains for what we use this index in our study. Such an introduction was requested by Reviewer 1 in the previous review process.

Line 135 Explain what you mean by “it should be relatively independent from statistical biases”. Historical records interpreted with quantitative or qualitative methods do have a bias, just different biases from a coral or proxy biased reconstruction. See Paleoclimatology textbook by Bradley 2015 and the chapter on Historical reconstructions and Garcia-Herrera, R., Konnen, G., Wheeler, D., Prieto, M., Jones, P. & Koek, F. 2005: CLIWOC: A Climatological Database for the World's Oceans 1750-1854. Climatic Change 73, 1. and Ingram, M. J., Underhill, D. J. & Wigley, T. M. L. 1978: Historical climatology. Nature 276, 329-334, http://dx.doi.org/10.1038/276329a0.

(l. 138) We agree with the reviewer and consequently revised the sentence.

Line 138-140 This sentence is redundant and not needed here but in the methods or results section, Delete or move “We use both indices by Quinn (1993) and Brönnimann et al. (2007) for identifying past warm and cold events in each coral record and we use these events to compile composites (see section 4.5).”

(l. 141) We will not delete this sentence, because it explains for what we use which index in our study. Such introduction was requested by Reviewer 1 in the previous review process.

Line 150 Check this exposure time for the x-ray process, this is a really long time. It usually takes a fraction of a second unless this is an ancient machine. If you used digital plates for the X-ray, I doubt the exposure time is that long.

(l. 152) We checked the exposure time. The exposure time for the X-ray machine we used is indeed 1-2 minutes. This produces very good X-ray images as it can be seen in the corresponding figures we provided in the supplementary material.

Note that the exposure time depends on the amperage, which can be determined by the user. Decreasing the amperage increases the exposure time, but from our experience this can help to produce better X-ray images (it is easier to optimize longer exposure times to best visualize the density bands of a coral slab).

Line 200 The reference Groth and Ghil (2015) is for a Monte Carlo Singular Spectrum Analysis (SSA) not wavelet coherence. Please use the correct reference for Wavelet coherence, Grinsted et al. (2004) doi:10.5194/npg-11-561-2004 is the one I use.

(l. 204) Thank you for pointing this out. We corrected the reference.

Line 210 You mean “section” not “chapter”. This is not a book or dissertation.

(l. 207 + 212) Revised.

Line 212-213 Eq. 1 The equation should be divided by the square root of the degrees of freedom. Data with sinusoidal cycles is not independent and violates the assumptions of many statistical tests. Your “n” values should be adjusted for degrees of freedom. It takes only two terms to define a sinusoid, the wave height, and length (or period), thus two degrees of freedom. If you have 15 years of data with a seasonal cycle, the degrees of freedom should be about 30. There are quantitative methods to determine your degrees of freedom, Runs test is the simplest dof test for a single data series and it is non-parametric. This adjustment is important because the larger your n values, the smaller your error, therefore, if you use unadjusted n values, your analysis could result in false positives.

(l. 216) We do not agree with the reviewer, because we do not apply Eq. 1 to data following a sinusoidal cycle. As stated in lines 212/213 Eq. 1 is applied to the data of the composite records. Composites are used to evaluate temperature anomalies identified in the coral records after removing the sinusoidal seasonal cycle. Consequently, the temperature anomalies are not data with sinusoidal cycles.

However, as all data are biased their statistical evaluation has to account for theses biases, which we do with Eq. 1. As the reviewer states "the larger your n values, the smaller you error", we calculate the standard error (Eq. 1), which also considers n, and not only the standard deviation, which does not consider n. Using the standard error allows us to better asses the bias associated with small values of n.

Line 217 Revise for incorrect usage of which "…coral samples, that show a good…"

(l. 219) Revised.

Section 4.2 This is a short section with 9 lines of text, the two subsections are not needed.

(l. 228) Adjusted.

Table 2 Explain what median RSD% is, is this from your ICP-OES analysis? That is the only other place RSD has been mention up to line 226.

(l. 705) We added this information as a note to the table.

Line 230 The number of samples appears twice in the sentence, same for the other sentences for the other corals in this section. The two subsections basically put what is in table 2 into text. The reader can read the table. Tell the reader something else about your results, such as means and medians are the same, thus these corals are not biased towards one season. B8 has a different mean, this one reason we removed the mean from the coral Sr/Ca records. The ranges vary among the corals with E5 having the greatest range and E3 the smallest. Rewrite this whole section to be more informative. Table 2 is for your raw Sr/Ca data, do these statistics change after linear interpolation? That is more interesting to me.

(l. 228-240) We revised this paragraph and added the description of the results as suggested by the reviewer.

Leupold et al. (2019; https://doi.org/10.1029/2018GC007796) show that the statistics of raw Sr/Ca do not change after interpolation.

Line 241 Revise "Such decadal variability in the Indian Ocean is described in previous studies". Change tense and redundant in word usage.

(l. 242) Revised.

Line 245 How were the coral Sr/Ca records detrended? Linear trend, polynomial?

In the "point-to-point reply" to Reviewer 2 previously in the review process we already showed how the coral Sr/Ca records were detrended:

l. 112-114: "For detrending we used published methods by Mudelsee (2000; https://doi.org/10.1016/s0098-3004(99)00141-7) and Mudelsee 2009; https://doi.org/10.1140/epjst/e2009-01089-3). Detrending was necessary to compile the composite records."

l. 689-694: "These programs are able to remove not only linear trends (which was the case with E3 and GIM as it can be seen in Figure S7 of the revised version of the supplementary material), but

they find breakpoints in time series where long-term trends change and calculate linear functions for these periods which are used for subtracting these long-term trends from the original time series. For example, coral record E5 in Figure S7 shows 4 linear graphs in red that were calculated with these programs overlying the original time series."
(Please note that Fig. S7 is now Fig. S8 in the revised version of the supplementary material.)
This means, four and three long-term linear trends were subtracted from E5 (1675-1716) and B8 (1836-1867), respectively, and one long-term linear trend was subtracted from E3 (1870-1909) and as well as from GIM (1980-1995).
The published methods we used are cited in the supplementary methods section of the supplementary materials.

Line 247 Are the mean annual cycles determine from the detrended data? make this clear. Include a figure with the detrended coral Sr/Ca series so the reader can see how you detrended the data. "Mean annual cycles" is confusing, do you mean annual values or seasonal cycles. In line 248 the authors use "seasonal amplitudes in coral SST" that is clearer.
"Mean annual cycles" is a commonly used term in this kind of paleoclimate analysis. For a detailed explanation please refer to the interactive discussion of this manuscript, author comment 2 (AC2), page 6, lines 10-14.

Line 250 I could not find in the supplementary material and Fig. S6 where the "26-32% of the coral-SST variance" is explained. The section 8 in the supplementary material notes the SSA is done with monthly anomalies, so the seasonal cycle is already removed. To figure out the % variance in seasonal cycle. Take the variance of the monthly Sr/Ca (before detrending) – variance of the monthly Sr/Ca anomalies with the seasonal cycle removed. That is your % variance due to the seasonal cycle. Can do the same with before and after detrending.
The "26-32% of the coral-SST variance" is explained in the supplementary material, lines 61-63. SSA was performed with both original and detrended data. This is described in Section 6 of the supplementary material.

Line 271 State explicitly what is meant by "in recent periods".
(l. 273) Revised.

Line 269 How is an "anomaly events" events defined? >0.5ºC or something else? Give explicit details.
Line 290 (now line 292) of the manuscript explains how we interpret an anomaly event: "when the anomaly exceeds 1.5 standard deviations of the mean of each coral record…."

Line 290 Fig S7 is the detrending plot with the anomalies. Move this figure to the main paper.
We will not move this Figure S7 (now Fig. S8) to the main paper, because Fig. S8 visualizes an aspect of the methodological approach used but is not required to understand the approach nor the results of their discussion and interpretation.

Line 299 Revise "These sub-periods were selected because…"
(l. 301) Revised.

Line 400-411 "In summary…" this should be in the conclusion section.
The conclusion basically repeats lines 400-411. Conclusions should not have numerical results, that would be in the results or discussion section. I suggest just moving lines 400-411 to the conclusion and delete most of the present conclusion sentences.

There are quite a few citations in lines 400-411 (now 403-414) used to compare our findings with other work and to elaborate on the implications of the study. These features clearly identify these lines as part of the discussion. Furthermore, citations should not be used in the conclusions. Therefore, we will not move these lines to the conclusion section.
We do not agree that the conclusion basically repeats lines 400-411. In addition, the content of the conclusion can be clearly identified as a conclusion whereas lines 400-411 can be clearly identified as part of the discussion as has been shown above. Furthermore, while not every paper might have numerical results in its conclusion section, providing these kind of information is not completely unusual, as can be seen in some articles published in Climate of the Past (e.g. https://doi.org/10.5194/cp-16-523-2020, https://doi.org/10.5194/cp-16-299-2020, https://doi.org/10.5194/cp-16-1187-2020).

ENSO and internal sea surface temperature variability in the tropical Indian Ocean since 1675

Maike Leupold[1], Miriam Pfeiffer[2], Takaaki K. Watanabe[3], Lars Reuning[2], Dieter Garbe-Schönberg[2], Chuan-Chou Shen[4,5,6], Geert-Jan A. Brummer[7]

[1]EMR-Group, Geological Institute, RWTH Aachen University, Aachen, 52062, Germany
[2]Institute of Geosciences, Kiel University, Kiel, 24118, Germany
[3]Department of Natural History Sciences, Faculty of Science, Hokkaido University, Sapporo, 060-0810, Japan
[4]High-Precision Mass Spectrometry and Environment Change Laboratory (HISPEC), Department of Geosciences, National Taiwan University, Taipei, 10617, Taiwan ROC
[5]Research Center for Future Earth, National Taiwan University, Taipei, LC6L73, Taiwan ROC
[6]Global Change Research Center, National Taiwan University, Taipei, 10617, Taiwan, ROC
[7]Department of Ocean Systems, Royal Netherlands Institute for Sea Research (NIOZ), and Utrecht University, 1790 AB Den Burg, The Netherlands

Correspondence to: Maike Leupold (maike.leupold@emr.rwth-aachen.de)

Abstract. The dominant modes of climate variability on interannual timescales in the tropical Indian Ocean are the El Niño Southern Oscillation (ENSO) and the Indian Ocean Dipole. El Niño events have occurred more frequently during recent decades and it has been suggested that an asymmetric ENSO teleconnection (warming during El Niño events is stronger than cooling during La Niña events) caused the pronounced warming of the western Indian Ocean. In this study, we test this hypothesis using coral Sr/Ca records from the central Indian Ocean (Chagos Archipelago) to reconstruct past sea surface temperatures (SST) in time windows from the mid-Little Ice Age (1675-1716) to the present. Three sub-fossil massive *Porites* corals were dated to the 17-18th century (one coral) and the 19-20th century (two corals). Their records were compared with a published modern coral Sr/Ca record from the same site. All corals were sub-sampled at a monthly resolution for Sr/Ca measurements, which were measured using a simultaneous ICP-OES. Wavelet coherence analysis shows that interannual variability in the four coral records is driven by ENSO, suggesting that the ENSO-SST teleconnection in the central Indian Ocean was stationary since the 17th century. To determine the symmetry of El Niño and La Niña events, we compiled composite records of positive and negative ENSO-driven SST anomaly events. We find similar magnitudes of warm and cold anomalies indicating a symmetric ENSO response in the tropical Indian Ocean. This suggests that ENSO is not the main driver of central Indian Ocean warming.

1 Introduction

As the impacts of global climate change increase, paleoclimate research is more important than ever. The Indian Ocean is of major relevance to global ocean warming as it has been warming faster than any other ocean basin during the last century and is the largest contributor to the current rise of global mean sea surface temperatures (SST; Roxy et al., 2014). Depending on the SST dataset, warming in the Indian Ocean is highest in the Arabian Sea (Roxy et al., 2014) or in the central Indian Ocean (Roxy et al., 2020).

Tropical corals can be used to reconstruct past changes of environmental parameters, such as SST, by measuring Sr/Ca. They can help to determine changes in past climate variability. Most coral paleoclimate studies covering periods before 1900 conducted in the tropical Indian Ocean predominantly focused on $\delta^{18}O$ measurements (e.g., Abram et al., 2015; Charles et al., 2003; Cole et al., 2000; Nakamura, et al., 2011; Pfeiffer et al., 2004). Several studies included Sr/Ca measurements for SST reconstructions in the central tropical Indian Ocean (Pfeiffer et al., 2006; Pfeiffer et al., 2009; Storz et al., 2013; Zinke et al., 2016), while others focused on the western or the eastern Indian Ocean (Abram et al., 2003; Abram et al., 2020; Hennekam et al., 2018; Watanabe et al., 2019) and/or on corals sampled at only bimonthly (Zinke et al., 2004; Zinke et al., 2008) or annual resolution (Zinke et al., 2014; Zinke et al., 2015). The lack of monthly resolved coral Sr/Ca data from the central tropical Indian Ocean limits our understanding of its response to transregional interannual climate phenomena, as these climate phenomena are phase-locked to the seasonal cycle.

Past El Niño Southern Oscillation (ENSO) variability on seasonal and interannual timescales has been reconstructed using corals from different settings in the Pacific Ocean (e.g., Cobb et al., 2003; Cobb et al., 2013; Freund et al., 2019; Grothe et al., 2019; Lawman et al., 2020; Li et al., 2011), where ENSO has a strong influence on climate variability. Since the early 1980s strong ENSO events occurred more frequently compared to past centuries (Baker et al., 2008; Freund et al., 2019; Sagar et al., 2016). An intensification of future extreme El Niño and La Niña events under global warming is supported by paleoclimate studies using corals from the central tropical Pacific Ocean (Grothe et al., 2019). Although the influence of ENSO on climate variability is strongest in the tropical Pacific Ocean, oceanic and atmospheric parameters of the Indian Ocean are influenced by ENSO, as shown in coral-based SST reconstructions of ENSO variability (e.g., Marshall and McCulloch, 2001; Storz and Gischler, 2011; Zinke et al., 2004). Strong El Niño and La Niña events influence the tropical Indian Ocean and the existence of a stable SST-ENSO teleconnection between the Pacific and the Indian Ocean has been demonstrated in previous studies covering the late 19th and the 20th century (Charles et al., 1997; Cole et al., 2000; Pfeiffer and Dullo, 2006; Wieners et al., 2017). El Niño events cause basin-wide warming of the Indian Ocean in boreal winter (December-February), whereas La Niña events cause cooling (Roxy et al., 2014). However, it has been suggested that El Niño events have a stronger influence on the Indian Ocean SST than La Niña events, i.e. the warming during El Niño events is larger than the cooling during La Niña events (Roxy et al., 2014). Roxy et al. (2014) suggested that this asymmetric ENSO teleconnection is one reason for the warming of the western Indian Ocean since 1900. The positive skewness of SST in the ENSO region of the tropical Pacific is due to ENSO asymmetry, i.e. it reflects the fact that El Niño events are often stronger than La Niña events (An and Jin, 2004; Burgers and Stevenson, 1999). At teleconnected sites, such as the tropical Indian Ocean, the response to El Niño and La Niña events, respectively, may be asymmetric as well, as suggested by Roxy et al. (2014). However, teleconnected sites may also show a symmetric response to El Niño and La Niña events (e.g., Brönniman et al., 2007).

As the impact of ENSO on SST in the central Indian Ocean is recorded by coral Sr/Ca (e.g., Pfeiffer et al., 2006), we test the hypothesis of an asymmetric ENSO teleconnection as a driver of Indian Ocean warming during the 20th century. We develop coral Sr/Ca records from three sub-fossil massive *Porites* corals covering periods of the Little Ice Age (1675-1716, 1836-1867), and the mid-19th to early 20th century (1870-1909) as well as from a 20th century coral core (1880-1995) from the central Indian Ocean (Chagos Archipelago) to reconstruct past SST variability. In this study, the concept of 'asymmetric' and 'symmetric' ENSO teleconnection refers to the magnitudes of warming and cooling during El Niño and La Niña events., i.e. we examine whether Indian Ocean warming during El Niño events is stronger than cooling during La Niña events. First, we determine whether ENSO variability is recorded in all coral Sr/Ca records from Chagos, then we identify past warm and cold events in each coral record and compile composites of warm and cold events. We then compare the magnitudes of positive and negative ENSO-driven SST anomalies in the Chagos coral Sr/Ca records and discuss whether or not they provide evidence for an asymmetric ENSO teleconnection in the tropical Indian Ocean.

2 Regional setting

2.1 Location

The Chagos Archipelago is located in the tropical Indian Ocean (70-74° E; 4-8° S), about 500 km south of the Maldives. It consists of several atolls with islands, submerged and drowned atolls, and other submerged banks, including the Great Chagos Bank which is the world's largest atoll (Fig. 1). The Great Chagos Bank covers an area of 18.000 km^2 with eight islands totaling 445 ha of land. Its lagoon has a maximum depth of 84 m and a mean depth of 50 m. Due to its large size and submerged islands, water exchange with the open ocean is substantial. The Salomon atoll is located about 135 km towards the northeast of Eagle Island. Its atoll area is about 38 km^2 and has an enclosed lagoon and an island area of more than 300 ha. The greatest depth of its lagoon is 33 m, with a mean depth of 25 m.

2.2 Climate

Chagos is situated in a region characterized by monsoon climate (Sheppard et al., 2012). The Northeast monsoon in austral summer is the wet season, and lasts from October to February (Pfeiffer et al., 2004). Light to moderate north-west trades blow. From April to October, strong winds from the southeast dominate (Sheppard et al., 1999).
Chagos lies at the eastern margin of the so-called Seychelles-Chagos thermocline ridge (SCTR). In the SCTR, a shallow thermocline causes open-ocean upwelling of cold waters. Upwelling along this region was first identified by McCreary et al. (1993) and is forced by both negative and positive wind stress curl (Hermes and Reason, 2009; McCreary et al., 1993). Compared to other upwelling regions in the Indian Ocean, the SST of the SCTR are relatively high (between 28.5°C and 30°C in austral summer). This causes very strong air-sea interactions (e.g., Hermes and Reason, 2008; Vialard et al., 2009).
On interannual timescales, the dominant mode of climate variability in the SCTR is the El Niño Southern Oscillation (ENSO). During El Niño events, the West Pacific warm pool is displaced towards the East resulting in cooler than normal SST in the

Western Pacific and basin-wide warming of the Indian Ocean (Izumo et al., 2014; Sheppard et al., 2013). Figure 2 compares the positive SST anomalies during El Niño events with the negative SST anomalies during La Niña events in the Indian and Pacific Ocean between 1982 and 2016, as inferred from 'Reynolds' OI v2 SST data (Reynolds et al., 2002; averaged over December-February). An ENSO response in the tropical Indian Ocean can be observed. However, this response is not as strong as it is in the Pacific Ocean.

Coupled ocean-atmosphere instabilities centered in the tropical Indian Ocean result in Indian Ocean Dipole (IOD) events (Saji et al., 1999; Sheppard et al., 2013; Webster et al., 1999). A negative (positive) IOD event is defined by warmer (cooler) than normal SST in the eastern part of the Indian Ocean and cooler (warmer) than normal SST in the western Indian Ocean. Several studies showed that the IOD is an inherent mode of variability of the Indian Ocean (e.g., Ashok et al., 2003; Krishnaswamy et al., 2015; Saji et al., 1999; Webster et al., 1999). The instrumental record of past IOD events does not go back further than 1960 (Saji and Yamagata, 2003). Coral-based reconstructions of past IOD events covering the past millennium suggest a recent intensification of the IOD (Abram et al., 2008; Abram et al., 2020). Those corals show few strong IOD events (i.e., 2019, 1997/98, 1961, 1877/78 and 1675), of which only three events (2019, 1961, 1675) occur independently of ENSO. Considering that an anomaly event recorded by corals can indicate both positive and negative IOD and El Niño and La Niña events, respectively, and that both phenomena tend to occur together (e.g., Luo et al., 2010; Saji and Yamagata, 2003), we decided to treat positive SST anomaly events found in our records as El Niño events even if they could be a result of IOD events independent from or co-occurring with El Niño and La Niña events.

2.3 Instrumental data

Analysis of SST determined from the Advanced Very High-Resolution Radiometer (AVHRR) satellite SST product (Casey et al., 2010) for the varying grid areas in Chagos [open ocean (72.13-72.63° E; 7.13-7.63° S) and lagoon (71.63-72.13° E; 5.13-5.63° S)] reveals different SST seasonality at Chagos depending on the reef setting (Fig. 3; cf. Leupold et al., 2019). At the open ocean reefs, where upwelling occurs, seasonal minima in SST are colder than in the lagoon, whereas maximum temperatures are not significantly different (t-value = 0.27; p-value = 0.79). Averaged over the entire area of the Chagos Archipelago (70-74° E; 4-8° S), SST are similar to SST measured in the lagoon. Long-term monthly SST anomalies (i.e., mean seasonal cycle removed) reveal that interannual SST anomalies, such as the El Niño event in 1997/98 or the La Niña event in 2010/11, have the same magnitude in both lagoon and open ocean settings (Fig. 3b). Both anomaly records are not significantly different (t-value = 0.34; p-value = 0.37). This suggests that the magnitudes of interannual signals at Chagos should be recorded consistently in all coral records analyzed in this study.

2.4 ENSO indices

The instrumental record of past El Niño and La Niña events is restricted to the late 19th and early 20th centuries. Reconstructions of past ENSO events differ depending on the statistics and/or proxies used (see e.g., Wilson et al., 2010 and

Brönnimann et al., 2007 for a discussion). Therefore, we compare our coral data with different ENSO indices presented briefly in the following. The study of Wilson et al. (2010) reconstructed an annually-resolved Niño3.4 index of past El Niño and La Niña events back to 1607, beyond the instrumental era, using data from the central Pacific (corals), the Texas-Mexico region of the United States of America (tree rings) and other regions in the Tropics (corals and an ice core), which we will refer to as the "Wilson Niño Index". We use the Wilson Niño Index for comparison with our coral SST records performing Wavelet Coherence Analysis in the time domain (see section 4.4). Data on the occurrence and magnitude of historical El Niño and La Niña events have been taken from Brönnimann et al. (2007). They combined several reconstructed ENSO indices, climate field reconstructions and early instrumental data, which were evaluated for consistency. Their reconstruction period extends back to 1500 (La Niña events) and 1511 (El Niño events), respectively. We also include the classical ENSO reconstruction of Quinn (1993) based on historical observations of various aspects of ENSO, which extends back until 1500. Both records (Brönnimann et al., 2007; Quinn, 1993) cover all our coral time windows, including our 17th century coral record. By including the original list of Quinn (1993), alongside with the updated list of Brönnimann et al. (2007), we aim to evaluate the sensitivity of our analysis to different ENSO reconstructions. We use both indices by Brönnimann et al. (2007) and Quinn (1993) for identifying past warm and cold events in each coral record that we then use to compile composites (see section 4.5).

3 Methods and materials

3.1 Coral collection and preparation

For this study, three sub-fossil coral samples were collected from boulder beaches and derelict buildings of former settlements at Chagos in February 2010 (Fig. S1). The sub-fossil corals record 41 years of a period from the mid-Little Ice Age (1675-1716), which coincides with the Maunder Minimum, a period of reduced sunspots observations (Eddy, 1976), 31 years of the late Little Ice Age (1836-1867) and 39 years of the mid-19th to early 20th century (1870-1909). Samples E3 (1870-1909) and E5 (1675-1716) were taken from Eagle Island (S 6°11.39'; E 71°19.58'), an island located on the western rim of the Great Chagos Bank (Fig. 1). Sample B8 (1836-1867) was taken from the lagoon-facing site of Boddam Island (S 5°21.56'; E 72°12.34') in the southwestern part of the Salomon Atoll. The samples were cross-sectioned into 0.7-1.0 cm thick slabs and X-rayed with a Faxitron X-ray model 43885 operated at 50 keV for 1-2 minutes and used together with a Konica-Minolta Regius ∑ RC 300 reader. From the slabs of each sub-fossil coral, powder samples were drilled at 1 mm increments using a micro-milling machine (type PROXXON FF 500 CNC). This depth resolution can be translated to monthly temporal resolution with average growth rates of 12 mm/yr. The subsampling paths were always set along the optimal growth axis that was determined based on X-ray images (Fig. S2).

Core GIM, a modern coral core, was included in the coral composite of the SCTR (Pfeiffer et al., 2017). This composite comprises cores from the Seychelles and Chagos. Additionally, the core top (1950-1995) of the GIM core has been calibrated with SST (Pfeiffer et al., 2009). Core GIM was drilled underwater in 1995 in the lagoon of Peros Banhos, located in the northwest of Chagos, from a living coral colony. The monthly coral Sr/Ca record of GIM extends from 1880-1995. Analytical procedures have been described in Pfeiffer et al. (2009). In this study, we use this core to estimate the magnitude of modern El Niño and La Niña events.

3.2 Coral Sr/Ca analysis

Sr/Ca measurements were performed at Kiel University using a Spectro Ciros CCD SOP inductively coupled plasma optical emission spectrometer (ICP-OES) following a combination of techniques described by Schrag (1999) and de Villiers et al. (2002). Elemental emission signals were simultaneously collected and subsequently drift corrected by sample-standard bracketing every six samples. Between 0.13 and 0.65 mg of coral powder was dissolved in 1.00 mL 0.2 M HNO_3. Before analysis, the solution was diluted with 0.2 M HNO3 to a final concentration of approximately 8 ppm Calcium. Strontium and Calcium intensity lines used are 421 nm and 317 nm, respectively. The intensities of Strontium and Calcium were converted into Sr/Ca ratios in mmol/mol. Before and after each measurement sequence (n = 448 measurements), a stack of 8 different reference materials, including international reference materials, JCp-1 and JCt-1 (Hathorne et al., 2013), were measured and used for calibration. For drift-correction, an in-house coral reference standard (Mayotte coral) was used. Average analytical precision of Sr/Ca determinations is 0.08% relative standard deviation (RSD) or 0.008 mmol/mol (n = 1973), translating into a temperature of around 0.1°C. The reproducibility of Sr/Ca ratios from multiple measurements both on the same day and on consecutive days is 0.08% RSD (n = 238; 1SD), translating into a temperature uncertainty of around 0.1°C.

3.3 Chronology

Each sub-fossil coral sample was dated by U-Th in 2016. U-Th isotopic measurements were performed with an MC-ICPMS (Thermo Electron Neptune) in the High-Precision Mass Spectrometry and Environment Change Laboratory (HISPEC) of the Department of Geosciences, National Taiwan University (NTU), following techniques described in Shen et al. (2012). U-Th isotopic compositions and concentrations are listed in Table 1.

Sample E5 covers the period from 1675 to 1716, herein further referred to as E5 (1675-1716). Sample B8 covers the period from 1836 to 1867, E3 from 1870 to 1909, both referred to as B8 (1836-1867) and E3 (1870-1909), respectively. The uncertainties of the age models are approximately ±1.9 years (E5), ±2.2 years (B8) and ±2.4 years (E3). All age models were verified by a second, independently measured U-Th age of each sample, measured in 2017 in the HISPEC laboratory of the Department of Geosciences, NTU, following techniques described in Shen et al. (2012). These age determinations are consistent with our Sr/Ca chronologies.

The chronology of the samples was developed based on seasonal cycles of coral Sr/Ca and by analyzing the density bands visible on X-ray images (Fig. S2). We assigned the highest Sr/Ca value to the SST minimum of each year and interpolated linearly between these anchor points to obtain a time series with equidistant time steps.

3.4 Diagenesis screening

A combination of X-ray diffraction (XRD) and optical as well as scanning electron microscopy (SEM) was used to investigate potential diagenetic alteration in the sub-fossil coral samples from Chagos that may have affected the Sr/Ca values (Figs. S3, S4, and S5). Representative samples for diagenesis screening were selected from all corals based on the X-ray images. For each coral sample, diagenetic modifications were analyzed using one thin-section, one sample for SEM, one 2-D-XRD measurement and one powder-XRD measurement. The 2-D-XRD system Bruker D8 ADVANCE GADDS at the Rheinisch-Westfaelische Technische Hochschule (RWTH) Aachen was used for non-destructive XRD point-measurements directly on thin-section blocks with a calcite detection limit of ~ 0.2 % (Smodej et al., 2015).

3.5 Statistics

All coral Sr/Ca records were centered, i.e. normalized with respect to their mean values (Pfeiffer et al., 2009), and translated into SST using a temperature dependence of -0.06 mmol/mol per 1°C for *Porites* corals at Chagos (Leupold et al., 2019; Pfeiffer et al., 2009).

Wavelet coherence plots between the coral Sr/Ca records and the Wilson Niño Index were generated using the *MATLAB* (version R2019b) software toolboxes by Grinstedt et al. (2004) to assess whether the interannual variability recorded in the corals is related to ENSO.

Composites of El Niño and La Niña events were generated by calculating the mean of positive and negative anomaly events taken from centered monthly coral SST anomaly records (see section 4.5). By centering the coral records to their mean and focusing on interannual variability, we eliminate the largest uncertainty of single-core Sr/Ca records, as shown by Sayani et al. (2019).

T-tests were conducted using the free web application *T-Test Calculator* (GraphPad QuickCalcs, 2019; https://www.graphpad.com/quickcalcs/ttest1/, last access: 09 April 2019). T-tests were used to determine if the mean values of two data sets, e.g. mean annual cycles in section 4.3 or mean anomalies of coral composites in section 4.5, are significantly different from each other.

As the significance of the monthly mean anomalies calculated for the composite records depends on the numbers of events, standard errors (SE) for monthly mean anomaly values were used and calculated as follows:

$$SE = \frac{standarddeviation(\sigma)}{\sqrt{Numberofevents(n)}}, \quad (1)$$

4 Results and Interpretation

4.1 Diagenesis

Only trace amounts of diagenetic phases were detected in the sub-fossil coral samples, that show a good to excellent preservation according to the criteria defined in Cobb et al. (2013). Isolated scalenohedral calcite cement crystals were observed in the thin-section of E5 (1675-1716) (Fig. S3 a-d). However, XRD results and SEM analysis confirm that the calcite abundance is below the detection limit of XRD (0.2%) in this sample (Fig. S3 e-f). B8 (1836-1867) shows trace amounts of patchily distributed, thin aragonite cement (Fig. S4). E3 (1870-1909) is devoid of diagenetic phases (Fig. S5), but in some areas of the thin-section dissolution of centers of calcification can be seen (Fig. S5 c-d). Slight dissolution and microborings are also visible with SEM (Fig. S5 f). However, microborings are always open and therefore will not influence the geochemistry. In summary, diagenesis screening revealed that the coral samples are suitable for conducting geochemical analysis and diagenetic modifications to the Sr/Ca records should be negligible.

4.2 Sr/Ca measurements

Table 2 gives an overview of the Sr/Ca ratios of each sub-fossil coral core and statistical key figures of the records. The monthly Sr/Ca time series are shown in Figure 4.

A total of 472 subsamples from E5 (1675-1716) was measured for Sr/Ca. The average Sr/Ca value is 8.96 ± 0.07 mmol/mol. The minimum Sr/Ca value over the 41-year sample span is 8.73 mmol/mol and the maximum value is 9.14 mmol/mol. From B8 (1836-1867), Sr/Ca ratios of 375 subsamples were measured. The average value is 9.02 ± 0.07 mmol/mol. The maximum Sr/Ca value for the 31-year sample span is 9.36 mmol/mol, the minimum Sr/Ca value is 8.85 mmol/mol. For E3 (1870-1909), Sr/Ca measurements were conducted on 415 subsamples. The average Sr/Ca value is 8.95 ± 0.06 mmol/mol for the 39-year sample span, with the minimum value being 8.79 mmol/mol and the maximum value being 9.17 mmol/mol.

The maximum ranges among the corals vary with E5 (1675-1716) having the greatest range and E3 (1870-1909) having the smallest one. It can be seen that mean and median values are the same, i.e. these corals are not biased towards one season. B8 (1836-1867) has a different mean than E5 (1675-1716) and E3 (1870-1909). This underlines the necessity to center the coral records to their mean to eliminate the uncertainty of single-core Sr/Ca records as explained in section 3.5.

4.3 Decadal variability and seasonal cycle

All coral SST records show variability on decadal scale (Fig. 4). This variability with a periodicity of 9-13 years was already described in previous studies of Indian Ocean corals (Charles et al., 1997; Cole et al., 2000; Pfeiffer et al., 2006; Pfeiffer et al., 2009; Zinke et al., 2008). Within a decadal cool (warm) phase, negative (positive) SST anomalies may occur. In particular, high-amplitude, short-term cool events are possible as Chagos lies in a region where open-ocean upwelling occurs (see Leupold et al., 2019). To ensure that decadal variability does not influence the composite records by inflating interannual warm or cool anomalies, decadal variability is removed by detrending the coral records.

The mean annual cycles of all sub-fossil coral SST records are not significantly different as indicated by p-values around 1 in the t-tests (Table 3, Fig. 4). The seasonal amplitudes in coral SST (°C) are slightly higher in E5 (1675-1716) (1.99°C) compared to B8 (1836-1867) (1.81°C) and E3 (1870-1909) (1.71°C). A shift of the seasonal temperature maximum from February (E5 and B8) to April (E3) can be observed (Fig. 4). Seasonal amplitudes explain 26-32% of the coral-SST variance (see supplementary material and Fig. S6).

4.4 ENSO signals in coral SST records

The modern and the sub-fossil coral SST records were compared with the annually resolved Wilson Niño Index that extends back until 1607 (Wilson et al., 2010). All coral records show positive and negative SST anomalies, which occur in years where El Niño and La Niña events have been reported (Fig. 5) and wavelet power spectra show significant interannual variability in the ENSO frequency band (Fig. S7). To analyze a possible correlation between the coral SST records and ENSO, Wavelet Coherence (WTC) was conducted on all coral records and the Wilson Niño Index (Wilson et al., 2010). Wavelet Coherence (WTC) plots were generated to find regions in time-frequency space where the Wilson Niño Index and the Chagos coral SST records co-vary, even if they do not have high power in those regions (Fig. 6).

All WTC plots of the Wilson Niño Index and coral SST records reveal time-localized areas of strong coherence occurring in periods that correspond to the characteristic ENSO cycles of two to eight years. The WTC plots for the Wilson Niño Index and the 19-20th century coral records show several regions where both time series co-vary. In contrast, the WTC plot of the Wilson Niño Index and the 17-18th century coral SST record shows only one region of co-variation at the beginning of the 18th century. The plots show that there is an approximate lag of nine months to one year between the 17-18th century coral SST record and the Wilson Niño Index (Fig. 6a), and a lag of approximate one to three years between B8 (1836-1867) and E3 (1870-1909) and the Wilson Niño Index, respectively, (Figs. 6b & c). However, the lags between the coral SST and the index time series are in the range of the age model uncertainties of the sub-fossil corals and do not represent real time-lags. For a further comparison of the coral SST records' and the Wilson Niño Index' frequencies, singular spectrum analysis and power spectra of non-detrended and detrended time series were computed (see supplementary material).

All coral records show anomaly events that can be explained with El Niño and La Niña events listed in Brönnimann et al. (2007) or Quinn (1993; Tables 4-6). Our results show that, compared to the 17-18th century, more El Niño and La Niña events per period are recorded in coral records of the central Indian Ocean during the late 20th century. According to the AVHRR satellite data and coral records, an El Niño event occurs on average every four years between 1981 and 2017 (AVHRR) or every five years between 1965 and 1995 (coral record), respectively (Tables 4-6). This is supported by the events listed in Quinn (1993) and reflects a change in ENSO frequency in the tropical Pacific. Overall, predominantly strong El Niño events are recorded by the coral records from Chagos, as indicated in the list of events presented in Brönnimann et al. (2007; Table 6). The number of events listed in Brönnimann et al. (2007) is comparable to the number of events recorded in the corals, whereas the number of events listed in Quinn (1993) is higher compared to the number of events recorded in the corals. The same holds for the negative SST anomaly events (La Niña and non-La Niña events): the number of La Niña events listed in Brönnimann et al. (2007) is similar to the number of negative anomaly events recorded in the coral records. Furthermore, negative anomaly events occurred every 2.6 years in the AVHRR data (1981-2017), every 6 years in the coral record (1965-1995) and every 5 years in Brönnimann et al. (2007; 1965-1995). During the 17-18th century, negative SST anomalies occurred every 6.8 years (coral record) or 10.3 years (Brönnimann et al., 2007; Tables 4-6).

4.5 ENSO composites

Composites of monthly coral SST anomalies were produced for El Niño and La Niña events to assess their magnitudes. Each composite was produced using coral records of several individual El Niño and La Niña events. An overview of the events used for generating each composite can be found in Table 4 and Table 5. An overview of all events found in the coral Sr/Ca records and of El Niño and La Niña events listed in Brönnimann et al. (2007) and Quinn (1993) for the studied time period is given in Table 6. Positive SST anomalies in the coral records were interpreted as El Niño events when (1) the year of occurrence was listed as an El Niño event in Brönnimann et al. (2007) and Quinn (1993) within the error of each coral age model and (2) when the anomaly exceeded 1.5 standard deviations of the mean of each coral record (Fig. S8). In addition to the strong La Niña events listed in Brönnimann et al. (2007), we added negative SST anomalies occurring in years after the El Niño events to the composite.

The composite record for El Niño events comprises 35 events, and 31 events are included in the La Niña composite (Table 4). To investigate changes in the magnitude of ENSO anomalies over time, composites for the time periods 17-18th century and 19-20th century, respectively, were generated. For the 17-18th century, six events (five events) were used for the El Niño (La Niña) composite. The composite for the 19-20th century includes events from the sub-fossil corals and the GIM record. In total, 29 events (26 events) were used for the El Niño (La Niña) composite. These 19-20th century composites, in turn, were split into three sub-periods: 1830-1929 (18 El Niño events, 16 La Niña events), 1930-1964 (five El Niño events, five La Niña events; Table 5) and 1965-1995 (six El Niño events, five La Niña events). These sub-periods were selected because ENSO activity was reduced between 1930 and 1965 compared to before 1930 and after 1965 (e.g., Cole et al., 1993).

Observations indicate that some upwelling events in the central Indian Ocean are not forced by large-scale ENSO or IOD variability but are associated with cyclonic wind stress curls in the southern tropical Indian Ocean (Dilmahamod et al., 2016; Hermes and Reason, 2009). Such an upwelling event occurred in August 2002 and was found in both the coral and satellite SST records at Chagos (see Leupold et al., 2019).

To investigate the potential effect of such negative anomaly events on the La Niña composites, the 19-20th century composites were split into composites of La Niña events and other negative anomaly events, which are not related to La Niña. La Niña and negative anomalies other than La Niña events were selected based on the months they occurred in, i.e. November-May (La Niña), June-September (Non-La Niña). As such events are also observed in the satellite era, we compared modern (1981-2018) satellite SST composites for El Niño events (nine events), La Niña events (10 events) and negative anomalies other than La Niña events (four events) with our coral SST composites. We used the AVHRR satellite SST (Casey et al., 2010) averaged over the entire Chagos Archipelago (4-8° S; 70-74° W).

4.5.1 Positive anomalies in coral and satellite SST composites

The central Indian Ocean coral composites of positive SST anomalies reveal higher SST anomalies during El Niño events compared to the satellite composites (Fig. 7), which may reflect the greater sensitivity of the corals to reef-scale temperatures

(Leupold et al., 2019) or the different time periods covered by these records (only two El Niño events in the AVHRR record overlap with the coral data). The coral composite of the 17-18th century shows higher anomalies than the coral composite of the 19-20th century (Fig. 7). All positive SST anomalies identified as El Niño events in the coral records show an average warming of 1.5 ± 0.1°C (n = 35; Fig. 7). The average positive temperature anomaly during El Niño events of the 17-18th century was 2.2 ± 0.2°C (n = 6), higher than and significantly different (p << 0.01) from the average positive El Niño temperature anomaly during the 19-20th century (1.3 ± 0.1°C; n = 29). The average positive temperature anomaly of El Niño events picked from the AVHRR satellite SST (covering the period from 1981 to 2018) of 0.8 ± 0.1°C (n = 9) is also lower than and significantly different (p << 0.01) from the average positive El Niño temperature anomaly in the 19-20th century. This suggests a greater impact of El Niño events on Indian Ocean SST during the 17-18th century compared to the 19-20th century and recent decades.

4.5.2 Negative anomalies in coral and satellite SST composites

No statistically significant differences were found between negative anomalies in coral SST in the central Indian Ocean during the 17-18th century and the 19-20th century and between La Niña and non-La Niña events (Fig. 8).
The composite including all negative SST anomalies identified as La Niña and non-La Niña events in the coral records shows an average negative SST anomaly of -1.6 ± 0.1°C (n = 31; Fig. 8). During the 19-20th century, the negative temperature anomaly for all La Niña events is -1.6 ± 0.1°C (n = 22) and for all non-La Niña events it is -1.5 ± 0.4°C (n = 9) (p = 0.75). La Niña events are slightly colder than non-La Niña events in the coral composites, but not statistically different (p = 0.60). The same is observed in the AVHRR satellite SST anomaly composites, where average negative La Niña temperature anomalies are -0.8 ± 0.1°C (n = 10) and non-La Niña anomalies are -0.6 ± 0.1°C (n = 4; p = 0.17).
The average negative temperature anomalies of La Niña and non-La Niña events during the 17-18th century were slightly less negative (-1.5 ± 0.3°C; n = 5), but not significantly different (p = 0.73) from the average negative temperature anomalies of the 19-20th century (-1.6 ± 0.2°C; n = 26).

4.5.3 Interannual SST anomalies during the 19th and 20th century

Dividing the 19-20th century into three sub-periods (1830-1929; 1930-1964; 1965-1995) and compiling SST anomaly composites allowed us to assess changes in the magnitude of ENSO-driven warm and cold anomalies over time (Fig. 9). The El Niño composites do not show systematic changes during the 19-20th century in the Indian Ocean. For the period between 1830 and 1929, the average positive temperature anomaly is 1.4 ± 0.1°C (n = 18), while between 1930 and 1964 the average positive temperature anomaly of 1.2 ± 0.1°C (n = 5) is slightly lower than in the previous period, but not significantly different (p = 0.5). For the last period of the 20th century, 1965 to 1995, the average positive temperature anomaly is again 1.4 ± 0.1°C (n = 6; Fig. 9).
The magnitude of cooling during La Niña and non-La Niña events tends to reduce from 1830-1929 to 1965-1995 (Fig. 9). For the period between 1830 and 1929, the average negative temperature anomaly is -1.9 ± 0.2°C (n = 16). Between 1930 and

1964 the average negative temperature anomaly increases by 0.58°C to -1.3 ± 0.1°C (n = 5), and from 1965 to 1995, the average negative temperature anomaly is -1.1 ± 0.1°C (n = 5). However, for both El Niño and La Niña events, the differences between the means of the first period (1830-1929) and the last period (1965-1995) are not statistically significant (p = 0.93; p = 0.07, respectively).

5 Discussion

Previous studies have shown that Indian Ocean SST variability was influenced by ENSO during the 19th and 20th centuries (Charles et al., 1997; Cole et al., 2000). During this period there was a stationary ENSO-SST teleconnection, in the sense that El Niño warmed the Indian Ocean and La Niña cooled it (Pfeiffer and Dullo, 2006). In this study, we show that interannual SST variability recorded in the 17-18th and 19-20th century corals is coherent with the Wilson Niño Index. This demonstrates a stationary ENSO-SST teleconnection in the central Indian Ocean since 1675.

Our ENSO composites allow us to estimate and compare the magnitudes of ENSO-induced warming and cooling in the central Indian Ocean. This enables us to assess the symmetry or asymmetry of the ENSO teleconnection, hence taking the analysis of the ENSO-SST teleconnection one step further. The composites suggest the ENSO teleconnection in the tropical Indian Ocean was close to symmetric, because magnitudes of El Niño and La Niña events recorded by the Chagos corals during the past century are in general comparable (Fig. 9). Only in times of cooler mean climates (i.e., during the 17-18th century), the corals seem to indicate higher amplitude ENSO-induced warm anomalies in the tropical Indian Ocean, although these differences are not statistically significant. Hence, our results do not support the notion that an asymmetric ENSO teleconnection with strong warming during El Niño years drives the recent warming of the tropical Indian Ocean as suggested by Roxy et al. (2014).

The modern coral records from the central Indian Ocean all show steady warming during the 20th century, and this warming also continues in the period of reduced ENSO activity between 1930 and 1965 (e.g., Abram et al., 2016; Charles et al., 1997; Pfeiffer and Dullo, 2006). This suggests that neither the magnitude, nor the frequency of past El Niño events explain the centennial-scale warming of the Indian Ocean.

Previous studies classified El Niño and La Niña events (Tables 4 and 5) qualitatively, from “weak” to “very strong” (Brönnimann et al., 2007; Quinn, 1993; Table 6). All positive anomaly events recorded by the coral records presented in our study were identified in at least one of these two studies (Table 6). However, not every event listed in Brönnimann et al., 2007 and Quinn (1993) is recorded by the central Indian Ocean corals. Especially the number of events presented in Quinn (1993) is higher compared to the number of events recorded by the corals. In contrast, the number of events listed in Brönnimann et al. (2007) is similar to the number recorded by the corals (Table 6). Brönnimann et al. (2007) only listed strong events. This suggests that corals from the central Indian Ocean predominantly record strong events. As most ENSO reconstructions consistently record strong events (while weak to moderate events differ between reconstructions) our results do not depend on the choice of the ENSO reconstruction.

Our results show that El Niño events resulted in stronger SST anomalies in the central Indian Ocean during a cooler mean climate (i.e., during the 17-18th century). This is consistent with Zinke et al. (2004) who found the highest amplitude of interannual variations in the ENSO frequency band between 1645–1715 in a coral $\delta^{18}O$ record from Ifaty, Madagascar. To date, the Ifaty coral is the longest continuous coral record from the Indian Ocean with sub-seasonal resolution. Furthermore, these results are in line with a multi-core study of Pfeiffer et al., (2017). They also found larger amplitudes of ENSO-induced warm anomalies in the tropical Indian Ocean in the late 19th century, a time when mean SSTs in the tropical Indian Ocean were cooler than today.

Comparing both periods (17-18th and 19-20th century), the La Niña and non-La Niña cold events show no significant changes. This suggests a stable negative SST anomaly pattern in the Indian Ocean. There is ambiguity about the reason for this observation. However, the Indian Ocean is the warmest tropical Ocean, and its warmest waters tend to show a low spatial and temporal SST variability. In the western and central Indian Ocean, SSTs in the cold season show the strongest warming since 1900 (e.g., Leupold et al., 2019; Roxy et al., 2014), but also larger spatial and temporal SST variability at various scales (Leupold et al., 2019).

The corals from Chagos record upwelling events in boreal summer, which are independent of ENSO, poorly represented in satellite data of SST (see Leupold et al., 2019), and may result in the failure of the Indian monsoon. Such an upwelling event occurred for example in 2002 and led to a drought over the Indian subcontinent (Jayakumar and Gnanaseelan, 2012; Krishnan et al., 2006). At present, little is known about the frequency or magnitude of these events in past decades or centuries. Coral proxy data from Chagos thus allow us to better understand these non-La Niña upwelling events.

In contrast to the stationary teleconnection between ENSO and SST in the central Indian Ocean, previous studies have shown that the ENSO-precipitation teleconnection is non-stationary (Timm et al., 2005). The impact of ENSO on rainfall in the central Indian Ocean depends on mean SSTs, and these surpassed a critical threshold for atmospheric convection in the mid-1970s, strengthening the El Niño signal in rainfall. However, our study does not indicate an increase in the magnitude of El Niño-related SST anomalies following this shift compared to earlier time periods of strong ENSO activity.

This study confirms that the ENSO-SST teleconnection between the Pacific and the Indian Ocean has been stationary since 1675 and that it is possible to reconstruct the magnitude of interannual SST variations in the tropical Indian Ocean. This is of importance because so far there is no reliable high-resolution reconstruction of ENSO variability in the tropical Indian Ocean covering the periods investigated within this study. ENSO reconstructions from the equatorial Pacific cover the 20th century (1998 to 1886) (Cobb et al., 2001) and time windows from the past millennium: 928-961, 1149-1220, 1317-1464 and 1635-1703 (Cobb et al., 2003). Cobb et al. (2003) combined three overlapping coral records of the 14-15th century and five coral records of the 17-18th century. We have shown that this approach would be applicable to the tropical Indian Ocean as well, using sub-fossil corals from boulder beaches and historical buildings. If a more complete record of millennial-scale coral reconstructions from the tropical Pacific and the Indian Ocean becomes available, it will be possible to assess the ENSO teleconnection based on an analysis of the coral records from both oceans. This is important because recent studies have shown that the tropical Indian Ocean plays a pivotal role in the 20th-century global temperature rise (Funk et al., 2008; Pfeiffer et al., 2017; Roxy et al., 2014) and the processes driving this warming are not fully understood yet.

6 Conclusions

We have shown that the ENSO-SST relationship in the central Indian Ocean was stationary since the 17th century. All four studied coral records show interannual variability coherent with ENSO variability, but variations in the intensity of El Niño and La Niña-induced SST anomalies in the central Indian Ocean. El Niño events cause average positive anomalies of 2.2 ± 0.2°C (n = 6) during the 17-18th century and 1.3 ± 0.1°C (n = 29) during the 19-20th century, while La Niña events cause average negative anomalies of -1.5 ± 0.3°C (n = 5) during the 17-18th century and -1.6 ± 0.2°C (n = 26) during the 19-20th century in the central Indian Ocean. However, not all cooling events are related to La Niña events, but also to processes internal to the Indian Ocean causing negative anomalies of -1.5 ± 0.4°C (n = 7) during the 19-20th century. The magnitudes of El Niño and La Niña events during the last century are comparable, indicating a symmetric ENSO teleconnection. An asymmetric ENSO teleconnection being the cause for the overall warming of the central, tropical Indian Ocean appears therefore unlikely. However, we suggest compiling composite records of negative and positive SST anomaly events from additional sub-fossil Indian Ocean corals to further explore the ENSO-SST teleconnection, and how it varies spatially in cooler or warmer climatic intervals.

Author contribution: M.L. conceived the study, wrote the manuscript and produced all figures. M.P., L.R., T.K.W. and D.G.-S. helped with analyzing and interpreting the data. L.R. assessed the preservation of the coral samples. T.K.W., C.-C.S. and G.-J.B. helped with dating the samples and developing the age models. M.P. acquired the funding for this project, contributed feedback and helped refine the writing.

Competing interests: The authors declare that they have no competing interests.

Data and materials availability: All methods needed to evaluate the conclusions in the paper are present in the paper and/or the supplementary material. The data plotted in all figures will be available to the public over the Paleoclimatology Branch of NOAA's National Center for Environmental Information (NCEI) (http://www.ncdc.noaa.gov/data-access/paleoclimatology-data).

Acknowledgments: We thank Karen Bremer for laboratory assistance and the Deutsche Forschungsgemeinschaft (DFG) for funding the projects PF 676/2-1 and PF 676/3-1. Coral U-Th dating was supported by grants from the Science Vanguard Research Program of the Ministry of Science and Technology, Taiwan, ROC (108-2119-M-002-012), the Higher Education Sprout Project of the Ministry of Education, Taiwan, ROC (108L901001), and National Taiwan University (109L8926).

References

Abram, N. J., Gagan, M. K., McCulloch, M. T., Chappell, J., and Hantoro, W. S.: Coral reef death during the 1997 Indian Ocean Dipole linked to Indonesian wildfires, Science, 301(5635), 952-955, https://doi.org/10.1126/science.1083841, 2003.

Abram, N. J., Gagan, M. K., Cole, J. E., Hantoro, W. S., and Mudelsee, M.: Recent intensification of tropical climate variability in the Indian Ocean, Nat. Geosci., 1(12), 849, https://doi.org/10.1038/ngeo357, 2008.

Abram, N. J., Dixon, B. C., Rosevear, M. G., Plunkett, B., Gagan, M. K., Hantoro, W. S., and Phipps, S. J.: Optimized coral reconstructions of the Indian Ocean Dipole: An assessment of location and length considerations, Paleoceanogr. Paleocl., 30(10), 1391-1405, https://doi.org/10.1002/2015pa002810, 2015.

Abram, N. J., McGregor, H. V., Tierney, J. E., Evans, M. N., McKay, N. P., Kaufman, D. S., ... and Steig, E. J.: Early onset of industrial-era warming across the oceans and continents, Nature, 536(7617), 411, https://doi.org/10.1038/nature19082, 2016.

Abram, N. J., Wright, N. M., Ellis, B., Dixon, B. C., Wurtzel, J. B., England, M. H., … and Heslop, D.: Coupling of Indo-Pacific climate variability over the last millennium, Nature, 579, 385–392, https://doi.org/10.1038/s41586-020-2084-4, 2020.

An, S. I., and Jin, F. F.: Nonlinearity and asymmetry of ENSO, J. Climate, 17(12), 2399-2412, https://doi.org/10.1175/1520-0442(2004)017<2399:NAAOE>2.0.CO;2, 2004.

Ashok, K., Guan, Z., and Yamagata, T.: A look at the relationship between the ENSO and the Indian Ocean dipole, J. Meteorol. Soc. Jpn. Ser. II, 81(1), 41-56, https://doi.org/10.2151/jmsj.81.41, 2003.

Baker, A. C., Glynn, P. W., and Riegl, B.: Climate change and coral reef bleaching: An ecological assessment of long-term impacts, recovery trends and future outlook, Estuar. Coast. Shelf. S., 80(4), 435-471, https://doi.org/10.1016/j.ecss.2008.09.003, 2008.

Brönnimann, S., Xoplaki, E., Casty, C., Pauling, A., and Luterbacher, J.: ENSO influence on Europe during the last centuries, Clim. Dynam., 28(2-3), 181-197, https://doi.org/10.1007/s00382-006-0175-z, 2007.

Burgers, G., and Stephenson, D. B.: The “normality” of El Niño, Geophys. Res. Lett., 26(8), 1027-1030, https://doi.org/10.1029/1999GL900161, 1999.

Casey, K. S., Brandon, T. B., Cornillon, P. and Evans, R.: The Past, Present and Future of the AVHRR Pathfinder SST Program, in: Oceanography from Space, edited by: Barale, V., Gower, J. F. R., and Alberotanza, L., Springer, Dordrecht, NL, 273-287, https://doi.org/10.1007/978-90-481-8681-5_16, 2010.

Charles, C. D., Hunter, D. E., and Fairbanks, R. G.: Interaction between the ENSO and the Asian monsoon in a coral record of tropical climate, Science, 277(5328), 925-928, https://doi.org/10.1126/science.277.5328.925, 1997.

Charles, C. D., Cobb, K. M., Moore, M. D., and Fairbanks, R. G.: Monsoon-tropical ocean interaction in a network of coral records spanning the 20th century, Mar. Geol., 201. https://doi.org/10.1016/S0025-3227(03)00217-2, 2003.

Cobb, K. M., Charles, C. D., and Hunter, D. E.: A central tropical Pacific coral demonstrates Pacific, Indian, and Atlantic decadal climate connections, Geophys. Res. Lett., 28(11), 2209-2212, https://doi.org/10.1029/2001gl012919, 2001.

Cobb, K. M., Charles, C. D., Cheng, H., and Edwards, R. L.: El Niño/Southern Oscillation and tropical Pacific climate during the last millennium, Nature, 424(6946), 271, https://doi.org/10.1038/nature01779, 2003.

Cobb, K. M., Westphal, N., Sayani, H. R., Watson, J. T., Di Lorenzo, E., Cheng, H., ... and Charles, C. D.: Highly variable El Niño–Southern Oscillation throughout the Holocene, Science, 339(6115), 67-70, https://doi.org/10.1126/science.1228246, 2013.

Cole, J. E., Fairbanks, R. G., and Shen, G. T.: Recent variability in the Southern Oscillation: Isotopic results from a Tarawa Atoll coral, Science, 260(5115), 1790-1793, https://doi.org/10.1126/science.260.5115.1790, 1993.

Cole, J. E., Dunbar, R. B., McClanahan, T. R., and Muthiga, N. A.: Tropical Pacific forcing of decadal SST variability in the western Indian Ocean over the past two centuries, Science, 287(5453), 617-619, https://doi.org/10.1126/science.287.5453.617, 2000.

de Villiers, S., Greaves, M. and Elderfield, H.: An intensity ratio calibration method for the accurate determination of Mg/Ca and Sr/Ca of marine carbonates by ICP-AES, Geochem. Geophy. Geosy., 3(1), 1001, https://doi.org/10.1029/2001gc000169, 2002.

Dilmahamod, A. F., Hermes, J. C., and Reason, C. J. C.: Chlorophyll-a variability in the Seychelles–Chagos Thermocline Ridge: Analysis of a coupled biophysical model, J. Marine Syst., 154, 220-232, https://doi.org/10.1016/j.jmarsys.2015.10.011, 2016.

Eddy, J.A.: The Maunder Minimum, Science, 192(4245), 1189-1202, https://doi.org/10.1126/science.192.4245.1189, 1976.

Freund, M. B., Henley, B. J., Karoly, D. J., McGregor, H. V., Abram, N. J., and Dommenget, D.: Higher frequency of Central Pacific El Niño events in recent decades relative to past centuries, Nat. Geosci., 12, 450–455, https://doi.org/10.1038/s41561-019-0353-3, 2019.

Funk, C., Dettinger, M. D., Michaelsen, J. C., Verdin, J. P., Brown, M. E., Barlow, M., and Hoell, A.: Warming of the Indian Ocean threatens eastern and southern African food security but could be mitigated by agricultural development, P. Natl. Acad. Sci USA, 105(32), 11081-11086, https://doi.org/10.1073/pnas.0708196105, 2008.

GraphPad QuickCalcs: T-Test Calculator, Retrieved from https://www.graphpad.com/quickcalcs/ttest1/, last access: 09 April, 2019.

Grinsted, A., Moore, J. C., and Jevrejeva, S.: Application of the cross wavelet transform and wavelet coherence to geophysical time series, Nonlin. Processes Geophys., 11, 561–566, https://doi.org/10.5194/npg-11-561-2004, 2004.

Grothe, P. R., Cobb, K. M., Liguori, G., Di Lorenzo, E., Capotondi, A., Lu, … and Toth, L. T.: Enhanced El Niño–Southern Oscillation variability in recent decades. Geophys. Res. Lett., 46, https://doi.org/10.1029/2019GL083906, 2019.

Hathorne, E. C., Gagnon, A., Felis, T., Adkins, J., Asami, R., Boer, W., ... and Demenocal, P.: Interlaboratory study for coral Sr/Ca and other element/Ca ratio measurements. Geochem. Geophy. Geosy., 14(9), 3730-3750, https://doi.org/10.1002/ggge.20230, 2013.

Hennekam, R., Zinke, J., van Sebille, E., ten Have, M., Brummer, G.-J. A., & Reichart, G.-J.: Cocos (Keeling) corals reveal 200 Years of multidecadal modulation of southeast Indian Ocean hydrology by Indonesian throughflow, Paleoceanogr. Paleocl., 33, 48– 60. https://doi.org/10.1002/2017PA003181, 2018.

Hermes, J. C., and Reason, C. J. C.: Annual cycle of the South Indian Ocean (Seychelles-Chagos) thermocline ridge in a regional ocean model, J. Geophys. Res.-Oceans, 113(C4), https://doi.org/10.1029/2007jc004363, 2008.

Hermes, J. C., and Reason, C. J. C.: The sensitivity of the Seychelles–Chagos thermocline ridge to large-scale wind anomalies, ICES J. Mar. Sci., 66(7), 1455-1466, 2009.

Hiess, J., Condon, D. J., McLean, N., and Noble, S. R.: 238U/235U systematics in terrestrial uranium-bearing minerals, Science, 335(6076), 1610-1614, https://doi.org/10.1093/icesjms/fsp074, 2012.

Huang, B., Thorne, P. W., Banzon, V. F., Boyer, T., Chepurin, G., Lawrimore, J. H., ... and Zhang, H. M.: Extended reconstructed sea surface temperature, version 5 (ERSSTv5): upgrades, validations, and intercomparisons, J. Climate, 30(20), 8179-8205, https://doi.org/10.1175/jcli-d-16-0836.1, 2017.

Izumo, T., Lengaigne, M., Vialard, J., Luo, J. J., Yamagata, T., and Madec, G.: Influence of Indian Ocean Dipole and Pacific recharge on following year's El Niño: interdecadal robustness, Clim. Dynam., 42(1-2), 291-310, https://doi.org/10.1007/s00382-012-1628-1, 2014.

Jayakumar, A., and Gnanaseelan, C.: Anomalous intraseasonal events in the thermocline ridge region of Southern Tropical Indian Ocean and their regional impacts, J. Geophys. Res.-Oceans, 117(C3), https://doi.org/10.1029/2011jc007357, 2012.

Krishnan, R., Ramesh, K. V., Samala, B. K., Meyers, G., Slingo, J. M., and Fennessy, M. J.: Indian Ocean-monsoon coupled interactions and impending monsoon droughts, Geophys. Res. Lett., 33(8), https://doi.org/10.1029/2006gl025811, 2006.

Krishnaswamy, J., Vaidyanathan, S., Rajagopalan, B., Bonell, M., Sankaran, M., Bhalla, R. S., and Badiger, S.: Non-stationary and non-linear influence of ENSO and Indian Ocean Dipole on the variability of Indian monsoon rainfall and extreme rain events, Clim. Dynam., 45(1-2), 175-184, https://doi.org/10.1007/s00382-014-2288-0, 2015.

Lawman, A. E., Quinn, T. M., Partin,J. W., Thirumalai, K., Taylor, F., … and Shen, C.-C.: A century of reduced ENSO variability during the Medieval Climate Anomaly, Paleoceanogr. Paleocl., 35, https://doi.org/10.1029/2019PA003742, 2020.

Leupold, M., Pfeiffer, M., Garbe-Schönberg, D., and Sheppard, C.: Reef-scale-dependent response of massive Porites corals from the central Indian Ocean to prolonged thermal stress–evidence from coral Sr/Ca measurements, Geochem. Geophy. Geosy., 20(3). https://doi.org/10.1029/2018GC007796, 2019.

Li, J., Xie, S. P., Cook, E. R., Huang, G., D'arrigo, R., Liu, F., ... and Zheng, X. T.: Interdecadal modulation of El Niño amplitude during the past millennium, Nat. clim. change, 1(2), 114-118., https://doi.org/10.1038/nclimate1086, 2011.

Luo, J. J., Zhang, R., Behera, S. K., Masumoto, Y., Jin, F. F., Lukas, R., and Yamagata, T.: Interaction between El Niño and extreme Indian ocean dipole, J. Climate, 23(3), 726-742, https://doi.org/10.1175/2009jcli3104.1, 2010.

Marshall, J. F., & McCulloch, M. T.: Evidence of El Niño and the Indian Ocean Dipole from Sr/Ca derived SSTs for modern corals at Christmas Island, eastern Indian Ocean. Geophys. Res. Lett., 28(18), 3453-3456., 2001.

McCreary, J. P., Kundu, P. K., and Molinari, R. L.: A numerical investigation of dynamics, thermodynamics and mixed-layer processes in the Indian Ocean, Prog. Oceanogr., 31, 181–244, https://doi.org/10.1016/0079-6611(93)90002-u, 1993.

Nakamura, N., Kayanne, H., Iijima, H., McClanahan, T. R., Behera, S. K., and Yamagata, T.: Footprints of IOD and ENSO in the Kenyan coral record, Geophys. Res. Lett., 38(24), https://doi.org/10.1029/2011gl049877, 2011.

Pfeiffer, M., Dullo, W. C., and Eisenhauer, A.: Variability of the Intertropical Convergence Zone recorded in coral isotopic records from the central Indian Ocean (Chagos Archipelago), Quaternary Res., 61(3), 245-255, https://doi.org/10.1016/j.yqres.2004.02.009, 2004.

Pfeiffer, M., and Dullo, W. C.: Monsoon-induced cooling of the western equatorial Indian Ocean as recorded in coral oxygen isotope records from the Seychelles covering the period of 1840–1994 AD, Quaternary Sci. Rev., 25(9-10), 993-1009, https://doi.org/10.1016/j.quascirev.2005.11.005, 2006.

Pfeiffer, M., Timm, O., Dullo, W. C., and Garbe-Schönberg, D.: Paired coral Sr/Ca and $\delta^{18}O$ records from the Chagos Archipelago: Late twentieth century warming affects rainfall variability in the tropical Indian Ocean, Geology, 34(12), 1069-1072, https://doi.org/10.1130/g23162a.1, 2006.

Pfeiffer, M., Dullo, W. C., Zinke, J., and Garbe-Schönberg, D.: Three monthly coral Sr/Ca records from the Chagos Archipelago covering the period of 1950–1995 AD: reproducibility and implications for quantitative reconstructions of sea surface temperature variations, Int. J. Earth Sci., 98(1), 53-66, https://doi.org/10.1007/s00531-008-0326-z, 2009.

Pfeiffer, M., Zinke, J., Dullo, W. C., Garbe-Schönberg, D., Latif, M., and Weber, M. E.: Indian Ocean corals reveal crucial role of World War II bias for twentieth century warming estimates, Sci. Rep.-UK, 7(1), 14434, https://doi.org/10.1038/s41598-017-14352-6, 2017.

Quinn, W. H.: The large-scale ENSO event, the El Niño and other important regional features, Bull. Inst. fr. études andines, 22(1), 13-34, 1993.

Reynolds, R. W., Rayner, N. A., Smith, T. M., Stokes, D. C., and Wang, W.: An improved in situ and satellite SST analysis for climate, J. Climate, 15(13), 1609-1625, https://doi.org/10.1175/1520-0442(2002)015<1609:aiisas>2.0.co;2, 2002.

Roxy, M. K,, Ritika, K., Terray, P. and Masson, S.: The curious case of Indian Ocean warming, J. Climate 27(22), 8501–8509, https://doi.org/10.1175/JCLI-D-14-00471.1, 2014.

Roxy M. K., Gnanaseelan, C., Parekh, A., Chowdary, J. S., Singh, S., Modi, A., Kakatkar, R., Mohapatra, S., and Dhara, C.: Indian Ocean Warming, in: Assessment of Climate Change over the Indian Region, edited by: Krishnan, R., Sanjay, J., Gnanaseelan, C., Mujumdar, M., Kulkarni, A., and Chakraborty, S., Springer, Singapore, 191-206, 2020.

Sagar, N., Hetzinger, S., Pfeiffer, M., Masood Ahmad, S., Dullo, W. C., and Garbe-Schönberg, D.: High-resolution Sr/Ca ratios in a Porites lutea coral from Lakshadweep Archipelago, southeast Arabian Sea: An example from a region experiencing steady rise in the reef temperature, J. Geophys. Res.-Oceans, 121(1), 252-266, https://doi.org/10.1002/2015jc010821, 2016.

Saji, N. H., Goswami, B. N., Vinayachandran, P. N., and Yamagata, T.: A dipole mode in the tropical Indian Ocean, Nature, 401(6751), 360, https://doi.org/10.1038/43854, 1999.

Saji, N. H., and Yamagata, T.: Structure of SST and surface wind variability during Indian Ocean dipole mode events: COADS observations, J. Climate, 16(16), 2735-2751, https://doi.org/10.1175/1520-0442(2003)016<2735:sosasw>2.0.co;2, 2003.

Sayani, H. R., Cobb, K. M., DeLong, K., Hitt, N. T., and Druffel, E. R.: Intercolony $\delta^{18}O$ and Sr/Ca variability among Porites spp. corals at Palmyra Atoll: Toward more robust coral-based estimates of climate, Geochem. Geophy. Geosy., https://doi.org/10.1029/2019gc008420, 2019.

Schrag, D. P.: Rapid analysis of high-precision Sr/Ca ratios in corals and other marine carbonates, Paleoceanography, 14(2), 97-102, https://doi.org/10.1029/1998pa900025, 1999.

Shen, C. C., Cheng, H., Edwards, R. L., Moran, S. B., Edmonds, H. N., Hoff, J. A., and Thomas, R. B.: Measurement of attogram quantities of 231Pa in dissolved and particulate fractions of seawater by isotope dilution thermal ionization mass spectroscopy, Anal. Chem., 75(5), 1075-1079, https://doi.org/10.1021/ac026247r, 2003.

Shen, C. C., Wu, C. C., Cheng, H., Edwards, R. L., Hsieh, Y. T., Gallet, S., ... and Hori, M.: High-precision and high-resolution carbonate 230Th dating by MC-ICP-MS with SEM protocols, Geochim. Cosmochim. Acta, 99, 71-86, https://doi.org/10.1016/j.gca.2012.09.018, 2012.

Sheppard, C. R. C., Seaward, M. R. D., Klaus, R., and Topp, J. M. W.: The Chagos Archipelago: an introduction, in: Ecology of the Chagos Archipelago, edited by: Shepard, C. R. C., and Seaward, M. R. D., Westbury Academic & Scientific Publishing, Otley, UK, 1-20, 1999.

Sheppard, C. R. C., Ateweberhan, M., Bowen, B. W., Carr, P., Chen, C. A., Clubbe, C., ... and Gaither, M. R.: Reefs and islands of the Chagos Archipelago, Indian Ocean: why it is the world's largest no-take marine protected area, Aquat. Conserv., 22(2), 232-261, https://doi.org/10.1002/aqc.1248, 2012.

Sheppard, C. R. C., Bowen, B. W., Chen, A. C., Craig, M. T., Eble, J., Fitzsimmons, N., ... and Koldewey, H.: British Indian Ocean Territory (the Chagos Archipelago): setting, connections and the marine protected area, in: Coral Reefs of the United Kingdom Overseas Territories, Springer, Dordrecht, NL, 223-240, 2013.

Smodej, J., Reuning, L., Wollenberg, U., Zinke, J., Pfeiffer, M., and Kukla, P. A.: Two-dimensional X-ray diffraction as a tool for the rapid, nondestructive detection of low calcite quantities in aragonitic corals, Geochem. Geophy. Geosy., 16(10), 3778-3788, https://doi.org/10.1002/2015gc006009, 2015.

Storz, D., and Gischler, E.: Coral extension rates in the NW Indian Ocean I: reconstruction of 20th century SST variability and monsoon current strength. Geo-Mar. Lett., 31(3), 141-154., https://doi.org/10.1007/s00367-010-0221-z, 2011.

Storz, D., Gischler, E., Fiebig, J., Eisenhauer, A., and Garbe-Schönberg, D.: Evaluation of oxygen isotope and Sr/Ca ratios from a Maldivian scleractinian coral for reconstruction of climate variability in the northwestern Indian Ocean, Palaios, 28(1), 42-55, https://doi.org/10.2110/palo.2012.p12-034r, 2013.

Timm, O., Pfeiffer, M., and Dullo, W. C.: Nonstationary ENSO-precipitation teleconnection over the equatorial Indian Ocean documented in a coral from the Chagos Archipelago, Geophys. Res. Lett., 32(2), https://doi.org/10.1029/2004gl021738, 2005.

Vialard, J., Duvel, J. P., Mcphaden, M. J., Bouruet-Aubertot, P., Ward, B., Key, E., et al.: Cirene: air–sea interactions in the Seychelles–Chagos thermocline ridge region, B. Am. Meteorol. Soc., 90(1), 45-61, https://doi.org/10.1175/2008bams2499.1, 2009.

Watanabe, T. K., Watanabe, T., Yamazaki, A., Pfeiffer, M., and Claereboudt, M. R.: Oman coral $\delta^{18}O$ seawater record suggests that Western Indian Ocean upwelling uncouples from the Indian Ocean Dipole during the global-warming hiatus, Sci. Rep.-UK, 9(1), 1887, https://doi.org/10.1038/s41598-018-38429-y, 2019.

Webster, P. J., Moore, A. M., Loschnigg, J. P., and Leben, R. R.: Coupled ocean–atmosphere dynamics in the Indian Ocean during 1997–98, Nature, 401(6751), 356, https://doi.org/10.1038/43848, 1999.

Wieners, C. E., Dijkstra, H. A., and de Ruijter, W. P.: The Influence of the Indian Ocean on ENSO Stability and Flavor, J. Climate, 30(7), 2601-2620, https://doi.org/10.1175/jcli-d-16-0516.1, 2017.

Wilson, R., Cook, E., D'Arrigo, R., Riedwyl, N., Evans, M. N., Tudhope, A., and Allan, R.: Reconstructing ENSO: the influence of method, proxy data, climate forcing and teleconnections, J. Quaternary Sci., 25(1), 62-78, https://doi.org/10.1002/jqs.1297, 2010.

Zinke, J., Dullo, W.-C., Heiss, G.A., and Eisenhauer, A.: ENSO and Indian Ocean subtropical dipole variability is recorded in a coral record off southwest Madagascar for the period 1659 to 1995, Earth Planet. Sc. Lett., 228(1-2), 177-194, doi: 10.1016/j.epsl.2004.09.028, https://doi.org/10.1016/j.epsl.2004.09.028, 2004.

Zinke, J., Pfeiffer, M., Timm, O., Dullo, W.-C., Kroon, D., and Thomassin, B. A.: Mayotte coral reveals hydrological changes in the western Indian Ocean between 1881 and 1994, Geophys. Res. Lett., 35(23), https://doi.org/10.1029/2008gl035634, 2008.

Zinke, J., Rountrey, A., Feng, M., Xie, S. P., Dissard, D., Rankenburg, K., Lough, J., and McCulloch, M. T.: Corals record long-term Leeuwin Current variability including Ningaloo Niño/Niña since 1795, Nat. Commun., 5, 3607. https://doi.org/10.1038/ncomms4607, 2014.

Zinke, J., Hoell, A., Lough, J. M., Feng, M., Kuret, A. J., Clarke, H., Ricca, V., Rankenburg, K., and McCulloch, M. T.: Coral record of southeastern Indian Ocean marine heatwaves with intensified Western Pacific temperature gradient, Nat. Commun., 6, 8562. https://doi.org/10.1038/ncomms9562, 2015.

Zinke, J., Reuning, L., Pfeiffer, M., Wassenburg, J. A., Hardman, E., Jhangeer-Khan, R., Davies, G. R., Ng, C. K. C., and Kroon, D.: A sea surface temperature reconstruction for the southern Indian Ocean trade wind belt from corals in Rodrigues Island (19° S, 63° E), Biogeosciences, 13, 5827–5847, https://doi.org/10.5194/bg-13-5827-2016, 2016.

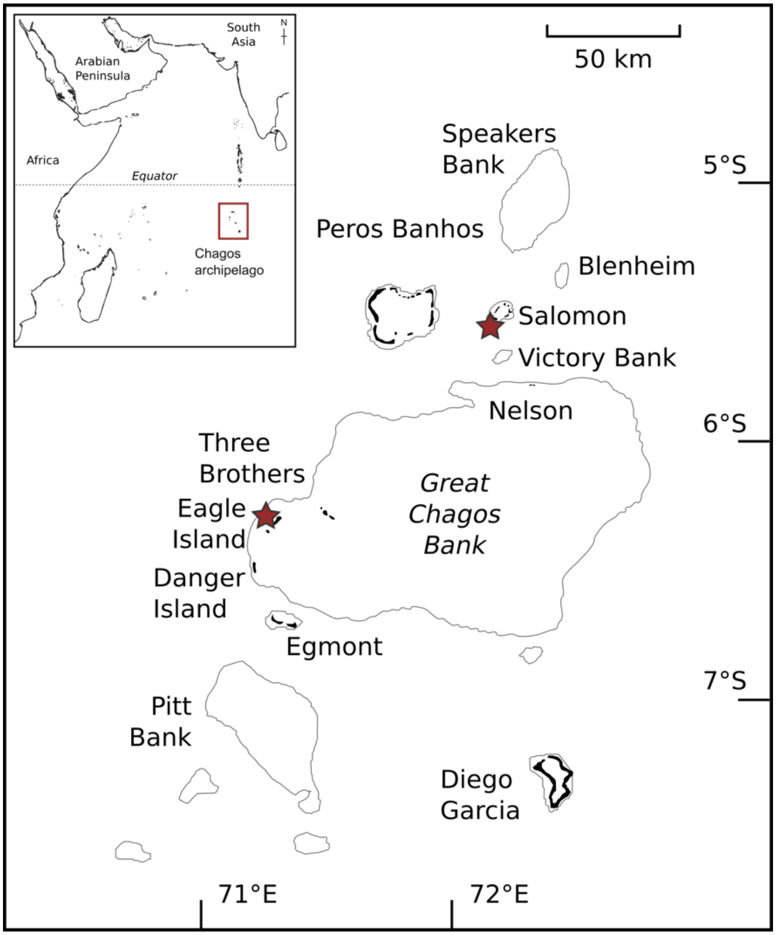

Figure 1: Location of study area and coral sample locations. The Chagos Archipelago is located in the central Indian Ocean, about 550 km south of the Maldives (map upper left). Fossil coral samples were collected on Eagle Island and on Boddam Island (Salomon atoll; red stars).

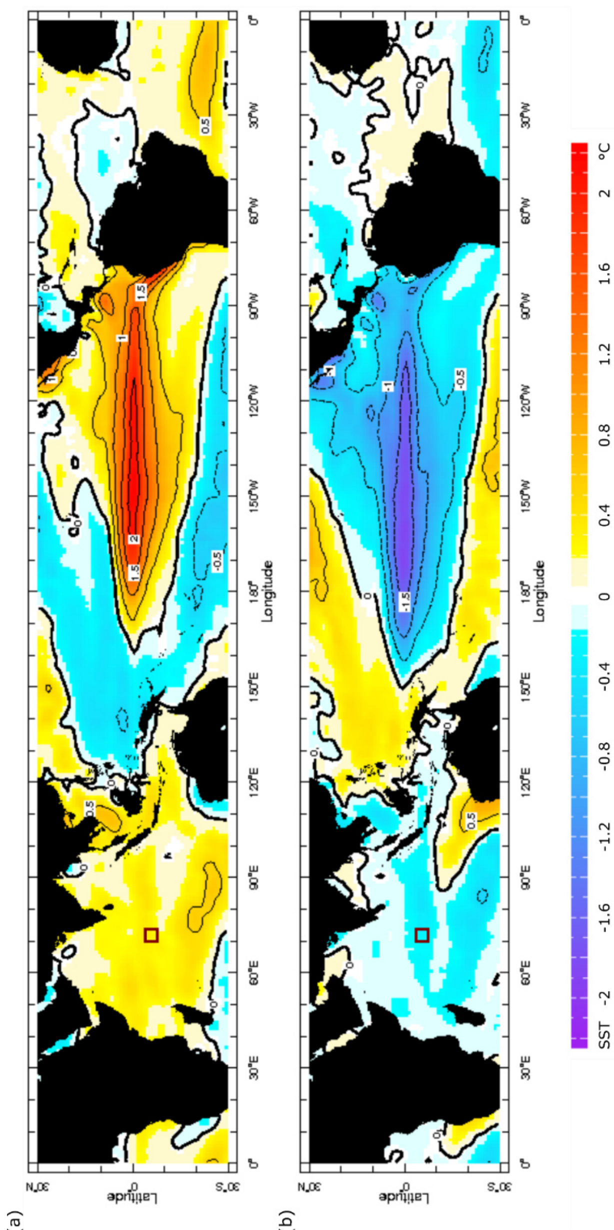

Figure 2: Composite maps of SST anomalies [°C] in the Indian and Pacific Ocean during El Niño and La Niña events. (a) El Niño SST anomalies for the period 1982 to 2016 averaged over December to February. (b) same as in (a), but for La Niña events. SST anomaly maps were computed with NOAA 'Reynolds' OI v2 SST (Reynolds et al., 2002) using the free web application Data Views of the IRI Data Library (https://iridl.ldeo.columbia.edu/). Date accessed: 17 September 2018. Red squares indicate the location of the study area. An overview of all events used for each composite map can be found in Table S1 in the supplementary material.

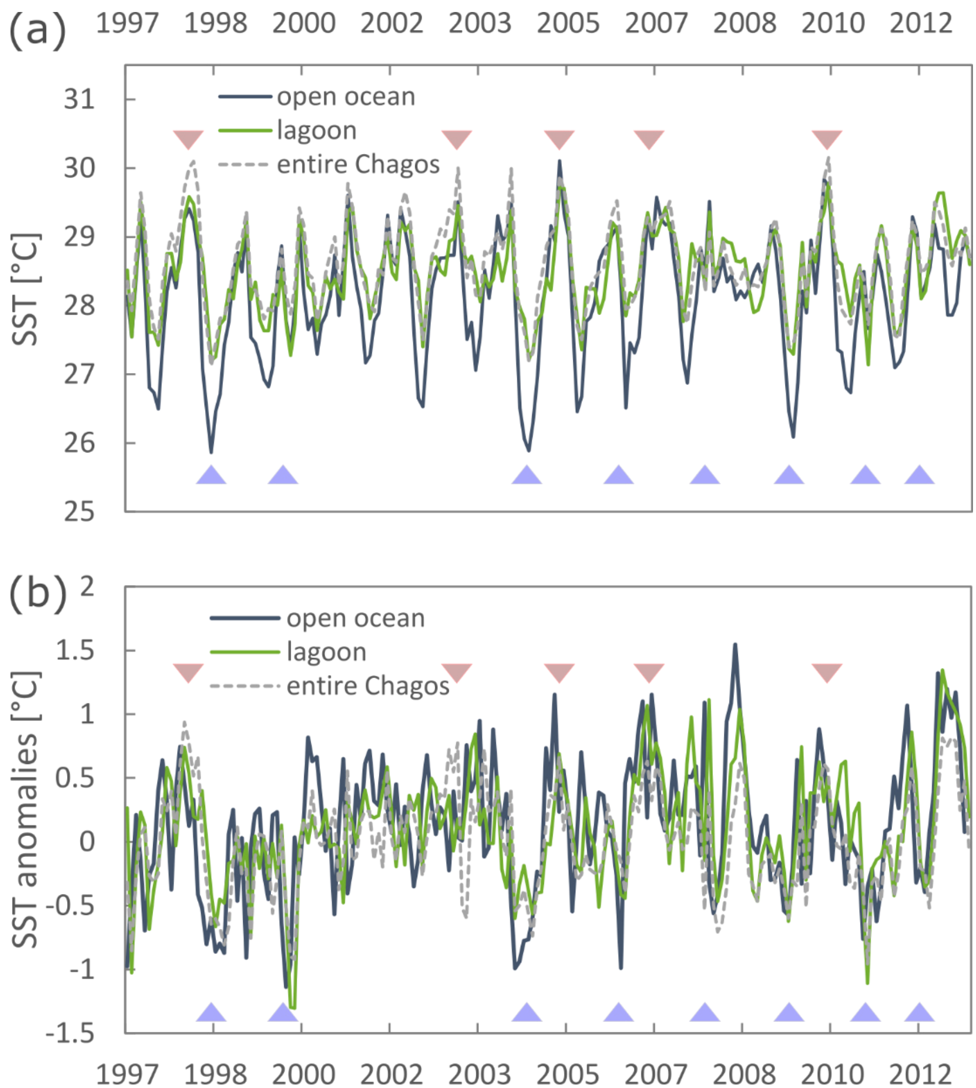

Figure 3: Satellite SST for different settings (lagoon: green; open ocean: dark blue) and the entire Chagos Archipelago (gray; averaged over 70-74° E; 4-8° S). (a) Monthly satellite SST means and (b) satellite SST anomalies. For the open ocean and lagoon setting we used the high-resolution satellite SST product AVHRR (Casey et al., 2010) and for the entire Chagos Archipelago we used NOAA 'Reynolds' OI v2 SST (Reynolds et al., 2002). Triangles indicate El Niño (red) and La Niña events (blue) based on Brönnimann et al. (2007) and the Oceanic Niño Index ONI (https://www.ggweather.com/enso/oni.htm; Date accessed: 18 October 2018).

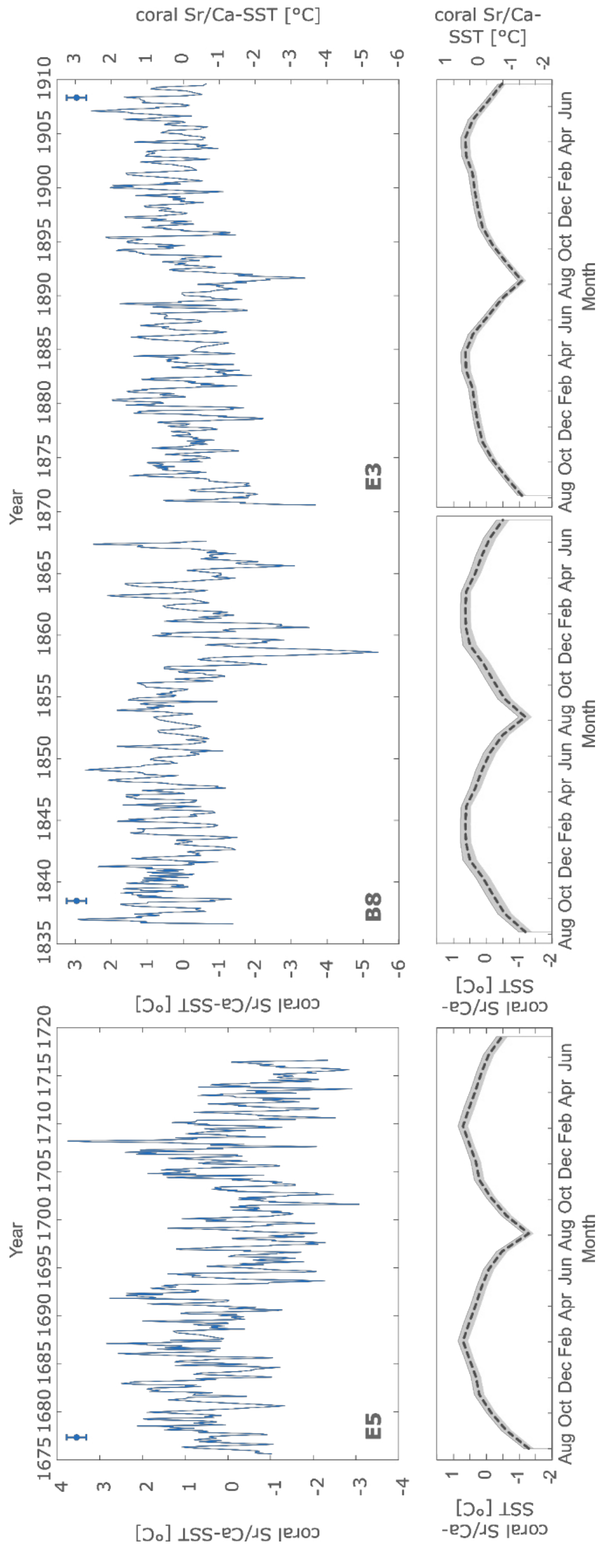

Year
coral Sr/Ca-SST [°C]
E3
B8
E5
Month
coral Sr/Ca-SST [°C]
Aug Oct Dec Feb Apr Jun Aug Oct Dec Feb Apr Jun

Figure 4: Monthly Sr/Ca records (blue lines; converted into coral Sr/Ca-SST in °C) of E5 (1675-1716), B8 (1836-1867) and E3 (1870-1909) with error bars indicating the standard deviation (±2σ) of Sr/Ca ratios from multiple measurements on the same day and on consecutive days and mean annual cycles (black lines and corresponding standard errors highlighted in gray, lower plot).

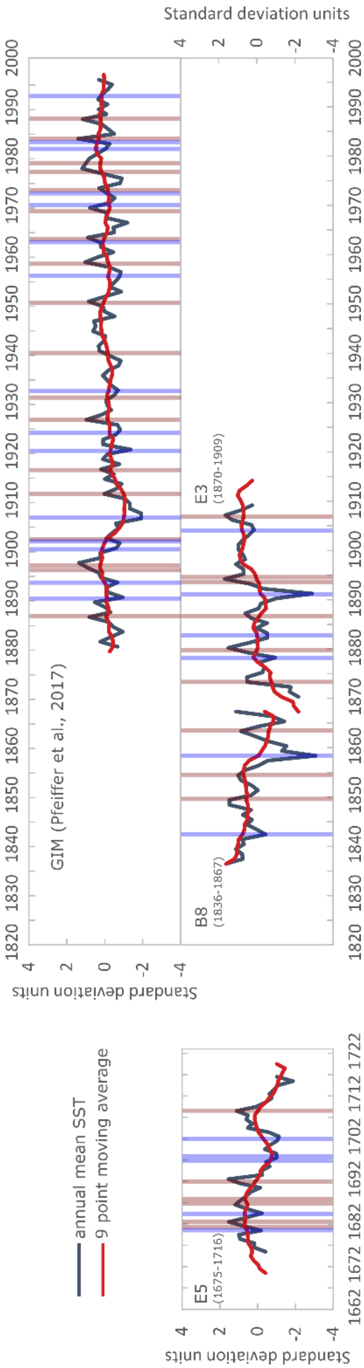

Figure 5: Annual SST anomalies for Chagos corals (this study and core GIM from Pfeiffer et al. 2009 and Pfeiffer et al., 2017) Red (El Niño) and blue (La Niña) shaded boxes indicate years used for the composite records (Figs. 7-9). Thick red lines are 9 point moving averages. See text Sect. 4.5 for how El Niño and La Niña events were picked.

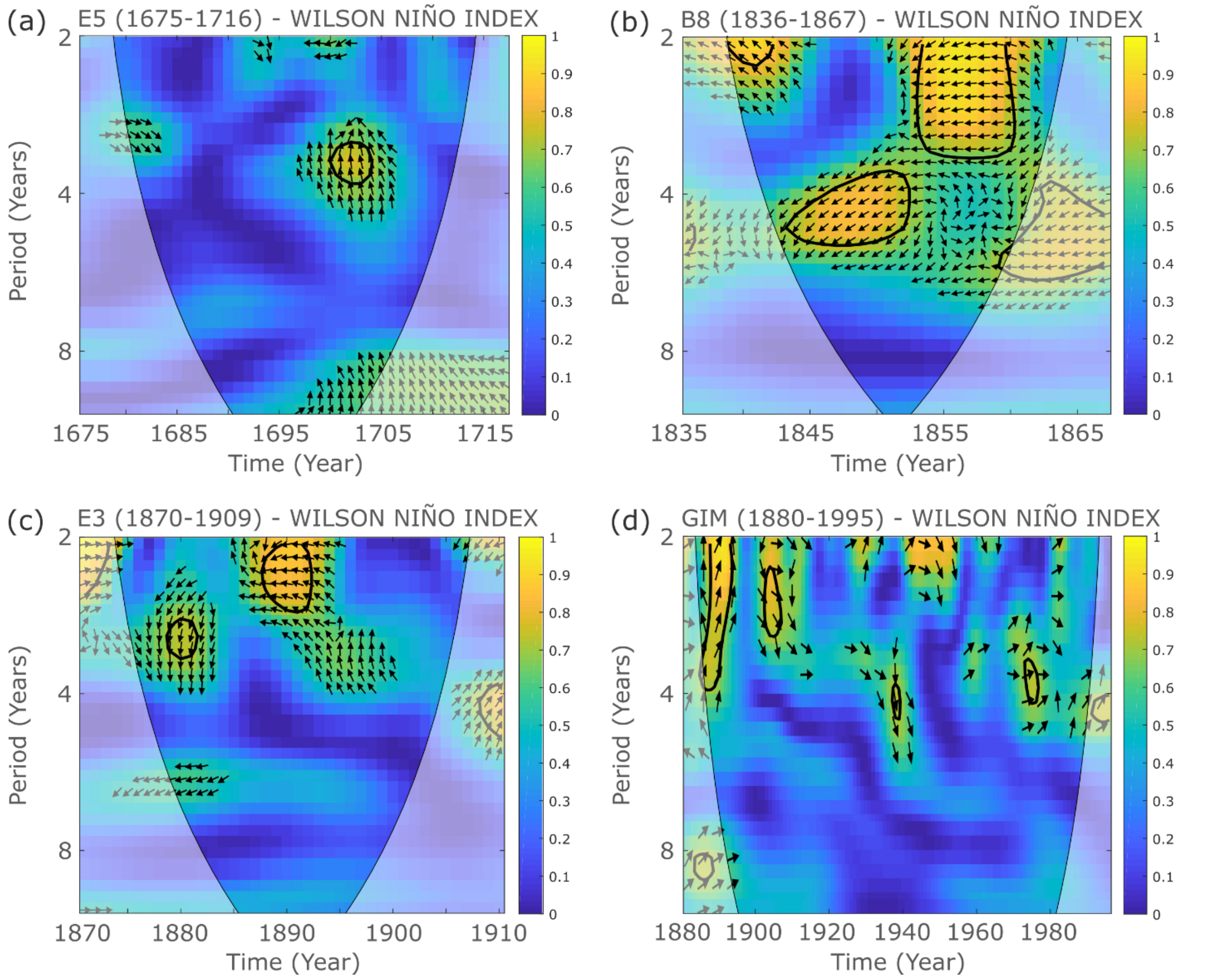

Figure 6: Wavelet coherence analysis plots for the Wilson Niño Index (Wilson et al., 2010) and Chagos coral SST of (a) E5 (1675-1716), (b) B8 (1836-1867), (c) E3 (1870-1909) and (d) GIM (1980-1995).

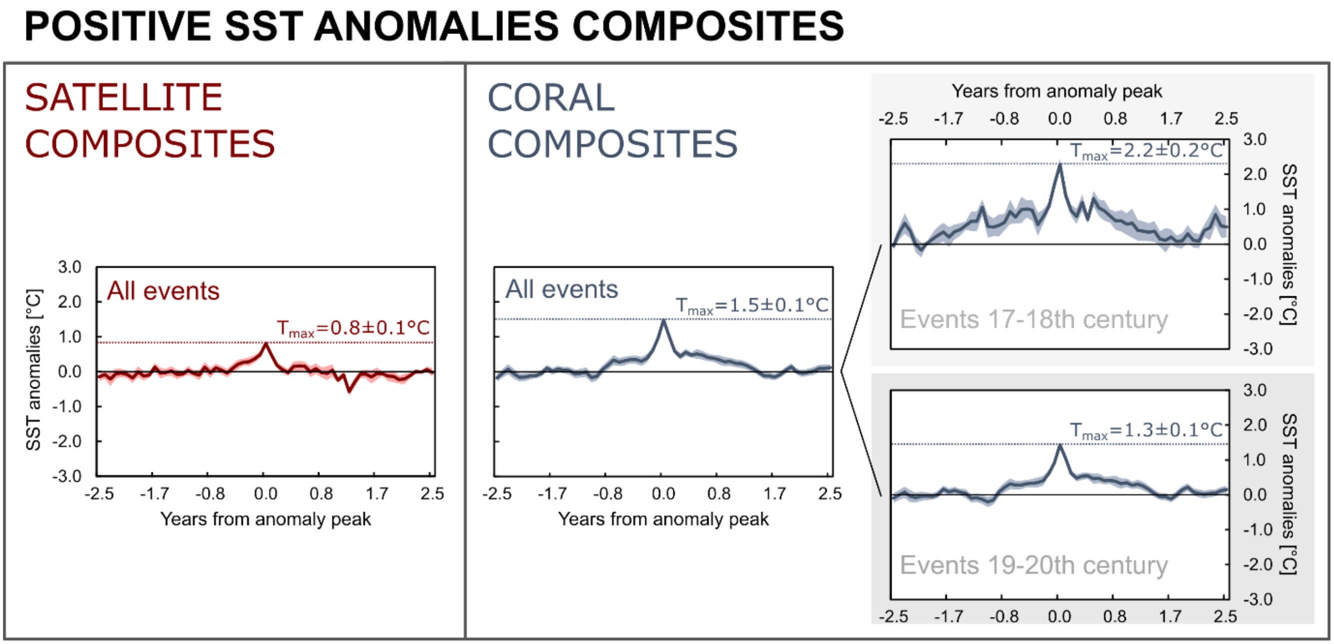

Figure 7: Positive SST anomalies (El Niño events) composite records of AVHRR (left; red) and coral SST (right; blue) records. Separate composites of anomaly events during the 17-18th and 19-20th century were generated from the coral SST records. Shaded areas below and above the curves show the standard error for the mean values of the composite records. See Table 4 for an overview
675 **of the events that were selected for generating the composites.**

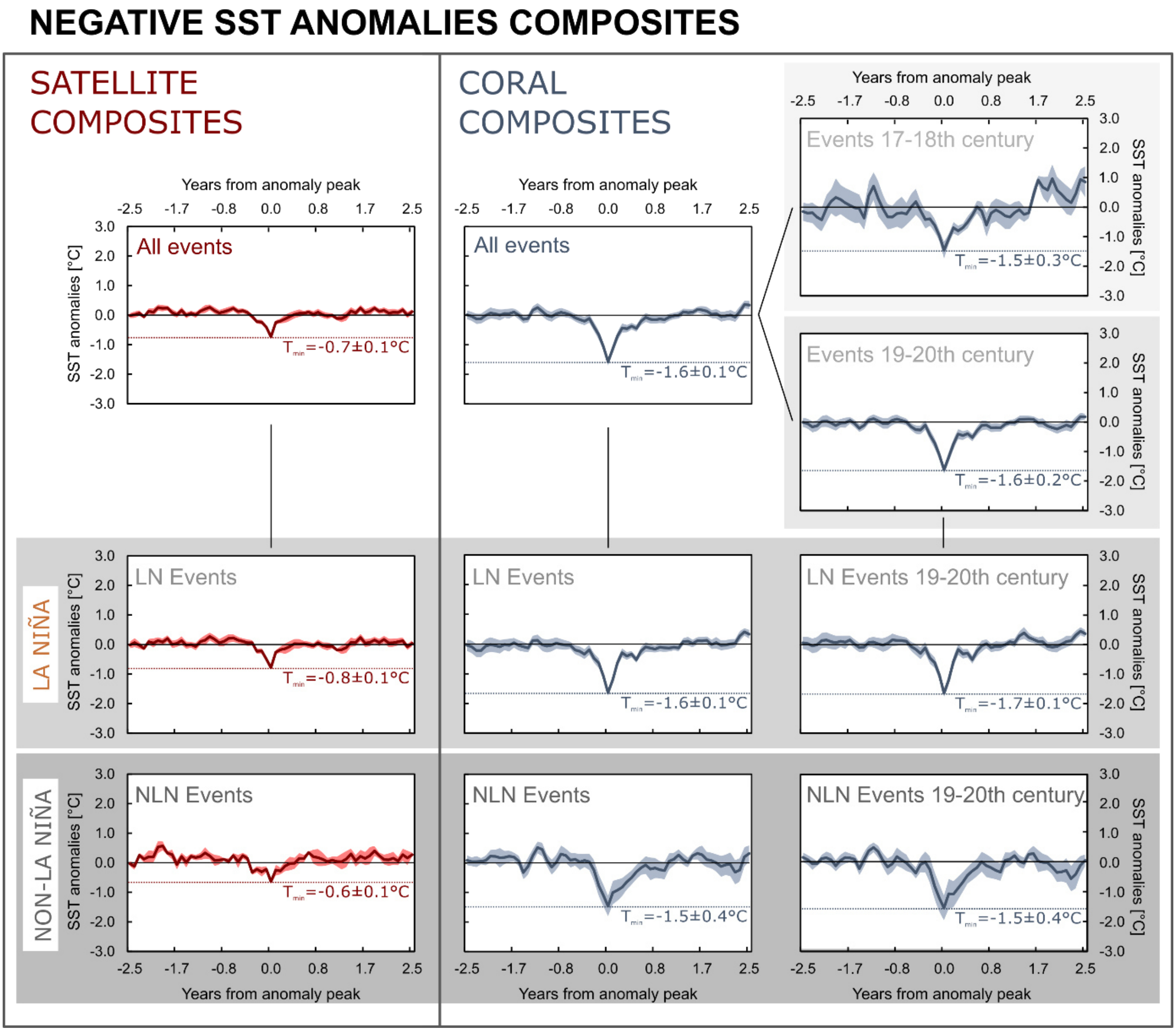

Figure 8: Negative SST anomalies (La Niña and non-La Niña events) composite records of AVHRR satellite (left; red) and coral SST (right; blue) records. Additionally, composites of anomaly events separated by 17-18th and 19-20th century events and by La Niña and non-La Niña events were generated. Shaded areas below and above the curves show the standard error for the mean values of the composite records. See Table 4 for an overview of the events that were selected for generating the composites.

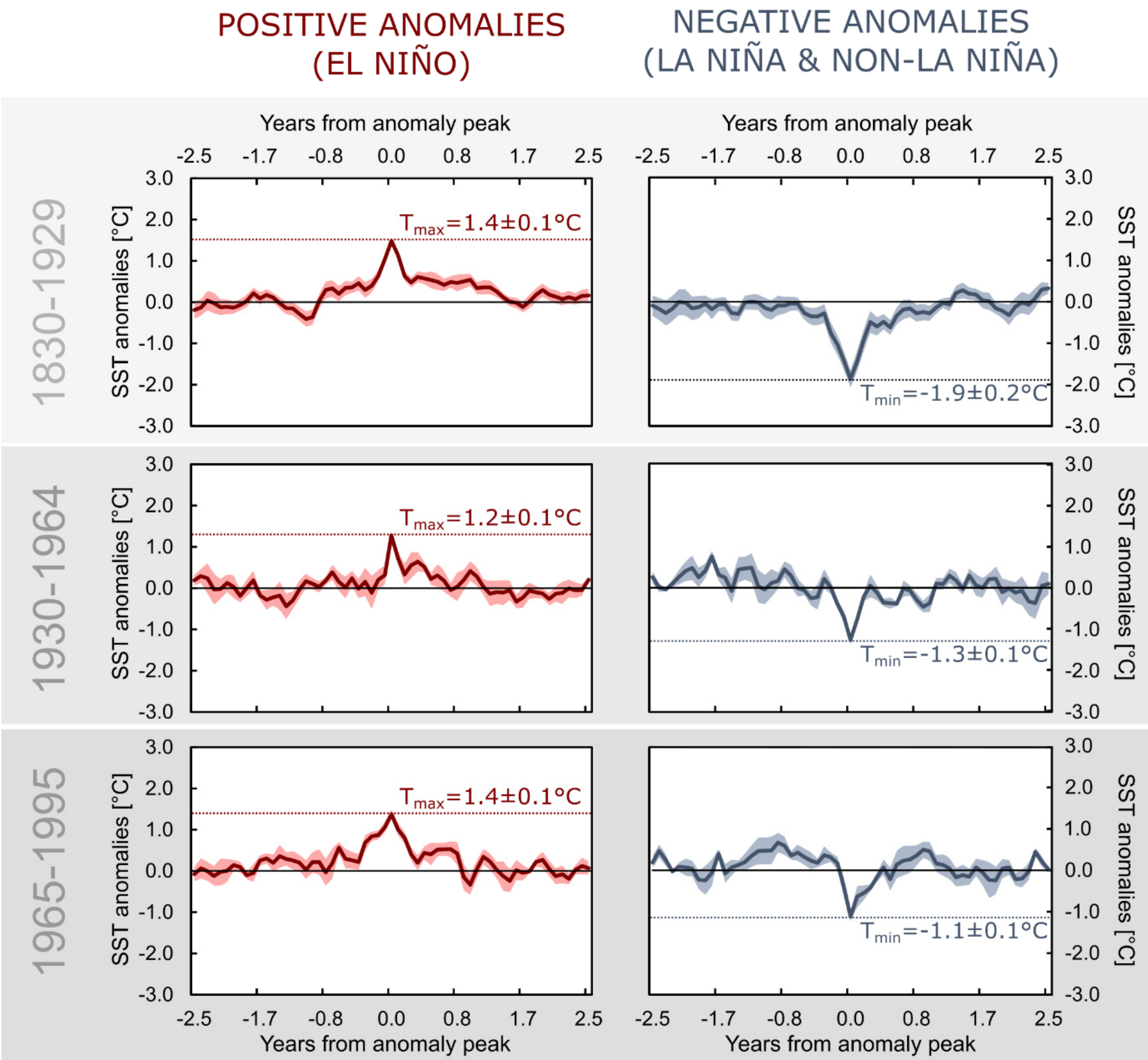

Figure 9: Positive (El Niño events; left) and negative SST anomalies (La Niña and non-La Niña events; right) composite records of the 19-20th century coral SST records separated by the time intervals 1830-1929 (top row), 1930-1964 (middle row) and 1965-1995 (bottom row). Shaded areas below and above the curves show the standard error for the mean values of the composite records. See Table 5 for an overview of the events that were selected for generating the composites.

Table 1: Overview of Uranium and Thorium isotopic compositions and ^{230}Th ages and corresponding years for fossil coral samples E5 (1675-1716), B8 (1836-1867) and E3 (1870-1909) measured with MC-ICP-MS, Thermo Electron Neptune, at NTU. Location of measurement numbers are indicated on X-ray images in Figure S2. Chemical analyses were performed on March, 11th, 2016 and on July 16, 2017 (Shen et al., 2003), and instrumental analysis on MC-ICP-MS (Shen et al., 2012).

Sample ID	Measurement No.	^{238}U (ppb^{a})	^{232}Th (ppt)	d^{234}U (measured^{a})	[$^{230}Th/^{238}U$] (activity^{c})	[$^{230}Th/^{232}Th$] (ppm^{d})	Age (uncorrected)	Age (corrected^{c,e})	d$^{234}U_{initial}$ (corrected^{b})	Corresponding year (BP)
E5 (1675-1716)	1st	2265,7 ±2,3	74,1 ±3,0	146,4 ±1,3	0,003250 ±0,000019	1639 ±66	309,5 ±1,9	308,8 ±1,9	146,6 ±1,3	1706 ± 1.9
	2nd	2293,9 ±2,2	16,1 ±1,3	145,0 ±1,6	0,003594 ±0,000018	8458 ±675	342,8 ±1,8	342,6 ±1,8	145,2 ±1,6	1674 ± 1.8
B8 (1836-1867)	1st	2212,7 ±2,5	37,1 ±4,1	144,1 ±1,5	0,001872 ±0,000023	1840 ±203	178,5 ±2,2	178,1 ±2,2	144,2 ±1,5	1838 ± 2.2
	2nd	2386,1 ±2,1	515,4 ±1,4	146,2 ±1,3	0,001650 ±0,000029	126 ±2	157,1 ±2,8	152,1 ±3,7	146,2 ±1,3	1865 ± 3.7
E3 (1870-1909)	1st	2551,9 ±2,5	56,7 ±3,9	145,4 ±1,3	0,001194 ±0,000025	886 ±64	113,8 ±2,4	113,3 ±2,4	145,4 ±1,3	1903 ± 2.4
	2nd	2694 ±2,8	643 ±2	144,7 ±1,7	0,0015 ±0,00002	106 ±1	146 ±2	141 ±3,2	145 ±1,7	1876 ± 3.2

Analytical errors are 2σ of the mean.

^{a}[^{238}U] = [^{235}U] x 137.818 (±0.65‰) (Hiess et al., 2012); $\delta^{234}U = ([^{234}U/^{238}U]_{activity} - 1) \times 1000$.

$^{b}\delta^{234}U_{initial}$ corrected was calculated based on ^{230}Th age (T), i.e., $\delta^{234}U_{initial} = \delta^{234}U_{measured} \times e^{\lambda 234 * T}$, and *T* is corrected age.

$^{c}[^{230}Th/^{238}U]_{activity} = 1 - e^{-\lambda 230 T} + (\delta^{234}U_{measured}/1000)[\lambda_{230}/(\lambda_{230} - \lambda_{234})](\lambda - e^{-(\lambda 230 - \lambda 234) T})$, where *T* is the age.

^{d}The degree of detrital ^{230}Th contamination is indicated by the [$^{230}Th/^{232}Th$] atomic ratio instead of the activity ratio.

^{e}Age corrections, relative to chemistry date, for samples were calculated using an estimated atomic $^{230}Th/^{232}Th$ ratio of 4 ± 2 ppm. Those are the values for a material at secular equilibrium, with the crustal $^{232}Th/^{238}U$ value of 3.8. The errors are arbitrarily assumed to be 50%.

Table 2: Statistical overview of raw Sr/Ca data.

Sample	Amount subsamples	Sr/Ca [mmol/mol]						median RSD [%]
		Mean	Median	Std dev	Min	Max	Range	
E5 (1675-1716)	472	8.96	8.96	0.07	8.73	9.14	0.410	0.076
B8 (1836-1867)	375	9.02	9.02	0.07	8.85	9.36	0.506	0.075
E3 (1870-1909)	415	8.95	8.95	0.06	8.79	9.17	0.376	0.074

***Note*: RSD is the relative standard deviation.**

Table 3: Statistical overview for mean annual cycle data of the coral Sr/Ca-SST [°C] records.

Sample	Max	Min	Amplitude	Mean	SD	P-value of t-test (two-tailed)		
						E5 (1675-1716) vs.	B8 (1836-1867) vs.	E3 (1870-1909) vs.
E5 (1675-1716)	0.70	-1.29	1.99	0.0026	0.5459		0.9979	0.9991
B8 (1836-1867)	0.61	-1.21	1.82	0.0033	0.5450	0.9979		0.9969

E3 (1870-1909)	0.60	-1.11	1.71	0.0024	0.5089	0.9991	0.9969

***Note*. SD is the standard deviation.**

	Composite		Years with events	Number of events	Records used
Positive SST anomalies	Coral Composites	all events	1679, 1682, 1686, 1687, 1691, 1708, 1849, 1853, 1863, 1873, 1879, 1881, 1886 (2x), 1889, 1894, 1895, 1896, 1897, 1902, 1907, 1911, 1916, 1926, 1932, 1940, 1951, 1958, 1963, 1969, 1973, 1977, 1979, 1983, 1987	35	E5 (1675-1716), B8 (1836-1867), E3 (1870-1909), GIM (1880-1995)
		17-18th century	1679, 1682, 1686, 1687, 1691, 1708	6	E5 (1675-1716)
		19-20th century	1849, 1853, 1863, 1873, 1879, 1881, 1886 (2x), 1889, 1894, 1895, 1896, 1897, 1902, 1907, 1911, 1916, 1926, 1932, 1940, 1951, 1958, 1963, 1969, 1973, 1977, 1979, 1983, 1987	29	B8 (1836-1867), E3 (1870-1909), GIM (1880-1995)
	Satellite Composite	all events	1983, 1987, 1988, 1998, 2003, 2005, 2007, 2015, 2016	9	AVHRR SST (1981-2018)
Negative SST anomalies	Coral Composites	all events	1680, 1684, 1697, 1698, 1702, 1846, 1858, 1860, 1865, 1872, 1883, 1890, 1891, 1893, 1895, 1900, 1902, 1903, 1906, 1920, 1924, 1932, 1947, 1952, 1956, 1964, 1970, 1974, 1982, 1984, 1994	31 (22 LN, 9 NLN)	E5 (1675-1716), B8 (1836-1867), E3 (1870-1909), GIM (1880-1995)
		17-18th century	1680, 1684, 1697, 1698, 1702	5	E5 (1675-1716)
		19-20th century	1846, 1858, 1860, 1865, 1872, 1883, 1890, 1891, 1893, 1895, 1900, 1902, 1903, 1906, 1920, 1924, 1932, 1947, 1952, 1956, 1964, 1970, 1974, 1982, 1984, 1994	26 (19 LN, 7 NLN)	B8 (1836-1867), E3 (1870-1909), GIM (1880-1995)
	Satellite Composite	all events	1984, 1989, 1989, 1992, 1995, 1996, 1998, 2000, 2004, 2008, 2011, 2012, 2014, 2017	14 (10 LN, 4 NLN)	AVHRR SST (1981-2018)

Table 4: Positive (El Niño events) and negative (La Niña, LN, and non-La Niña, NLN, events) SST anomaly events picked for generating coral and satellite composite records shown in Figure 7 and Figure 8.

19-20th century Coral Composite	Period	Years with events	Number of events	Records used
Positive SST anomalies	1830-1929	1849, 1853, 1863, 1873, 1879, 1981, 1886 (2x), 1889, 1894, 1895, 1896, 1897, 1902, 1907, 1911, 1916, 1926	18	B8 (1836-1867), E3 (1870-1909), GIM (1880-1995)
	1930-1964	1932, 1940, 1951, 1958, 1963	5	GIM (1880-1995)
	1965-1995	1969, 1973, 1977, 1979, 1983, 1987	6	GIM (1880-1995)
Negative SST anomalies	1830-1929	1846, 1858, 1860, 1865, 1872, 1883, 1890, 1891, 1893, 1895, 1900, 1902, 1903, 1906, 1920, 1924	16	B8 (1836-1867), E3 (1870-1909), GIM (1880-1995)
	1930-1964	1932, 1947, 1952, 1956, 1964	5	GIM (1880-1995)
	1965-1995	1970, 1974, 1982, 1984, 1994	5	GIM (1880-1995)

Table 5: 19-20th century (divided into three periods) positive (El Niño events) and negative (La Niña and non-La Niña events) SST anomaly events picked for generating coral composite records shown in Figure 9.

	Positive SST Anomalies						Negative SST Anomalies			
	Events in Records		Published ENSO events				Events in Records		Published ENSO events	
			Quinn (1993)		Brönnimann et al. (2007)				Brönnimann et al. (2007)	
	Years	Numbers of events	Years of very strong (VS), strong (S), medium (M) and weak (W) events	Numbers of events	Years of strong events	Numbers of events	Years	Numbers of events	Years of strong events	Numbers of events
E5 (1675-1716)	1678/79, 1682/83, 1685/86, 1686/87, 1691/92, 1707/08	6	1681 (S), 1684 (M+), 1687-88 (S+), 1692-93 (S), 1696-97 (M+), 1701 (S+), 1707-09 (M/S), 1715-16 (S)	8	1674, 1675, 1677, 1681, 1682, 1691, 1702	7	1680, 1683/84, 1697, 1697/98, 1702	5	1676, 1678, 1698, 1704	4
B8 (1836-1867)	1848/49, 1853/54, 1862/63	3	1837 (M+), 1844-46 (M/S+), 1850 (M), 1852 (M), 1854 (M), 1857-58 (M), 1860 (M), 1862 (M-), 1864 (S), 1866 (M+), 1867-68 (M+)	11	1833, 1846, 1852, 1856, 1869	5	1845/46, 1858, 1860/61, 1864/65	4	1842, 1847, 1863	3
E3 (1870-1909)	1872/73, 1879/80, 1885/86, 1893/94, 1894/95, 1906/07	6	1871 (S+), 1874 (M), 1877-78 (VS), 1880 (M), 1884 (S+), 1887-89 (M+), 1891 (VS), 1897 (M+), 1899-1900 (S), 1902 (M+), 1904-05 (M-), 1907 (M)	12	1869, 1877, 1878, 1889, 1897, 1900, 1903, 1906, 1912	9	1872, 1882/83, 1891, 1895/96, 1903/04	5	1872, 1887, 1890, 1893, 1904, 1910	6
GIM (1880-1995)*	1880/81, 1885/86, 1888/89, 1896/97, 1897, 1902, 1911/12, 1916/17, 1925/26, 1931/32, 1939/40, 1950/51, 1957/58, 1962/63, 1969/70, 1972/73, 1977/78, 1978/79, 1982/83, 1986/87	20	1880 (M), 1884 (S+), 1887-89 (M-/M+), 1891 (VS), 1897 (M+), 1899-90 (S), 1902 (M+), 1904-05 (M-), 1907 (M), 1910 (M+), 1911-12 (S), 1914-15 (M+), 1917 (S), 1923 (M), 1925-26 (VS), 1930-31 (M), 1932 (S), 1939 (M+), 1940-41 (S), 1943 (M+), 1951 (M-), 1953 (M+), 1957-58 (S), 1965 (M+), 1969 (M-), 1972-73 (S), 1976 (M), 1978-79 (W), 1982-83 (VS), 1987 (M), 1991-92 (M), 1994-95 (M-)	32	1878, 1889, 1897, 1900, 1903, 1906, 1912, 1915, 1919, 1926, 1931, 1940, 1941, 1952, 1958, 1966, 1973, 1977, 1983, 1987, 1992	21	1889/90, 1893, 1899/00, 1901/02, 1906, 1919/20, 1924, 1931/32, 1947, 1956, 1951/52, 1964, 1970, 1973/74, 1982, 1983/84, 1993/94	17	1887, 1890, 1893, 1904, 1910, 1917, 1925, 1934, 1943, 1950, 1956, 1968, 1971, 1974, 1976, 1985, 1989	17
AVHRR*	1982/83, 1986/87, 1987/88, 1997/98, 2002/03, 2004/05, 2006/07, 2014/15, 2015/16	9	1982/83 (VS), 1986/87 (M), 1987/88 (S), 1991/92 (S), 1994/95 (M), 1997/98 (VS), 2002/03 (M), 2004/05 (W), 2006/07 (W), 2009/10 (M), 2014/15 (W), 2015/16 (VS)	12	/	/	1984/85, 1989, 1989, 1992, 1995, 1996/97, 1998/99, 1999/00, 2004, 2007/08, 2010/11, 2011/12, 2014, 2016/17	14	1983/84 (W), 1984/85 (W), 1988/89 (S), 1992, 1995/96 (M), 1996/97, 1998/99 (S), 1999/00 (S), 2000/01 (W), 2004, 2005/06 (W), 2007/08 (S), 2008/09 (W), 2010/11 (S), 2011/12 (M), 2014, 2016/17 (W), 2017/18 (W)	18

* Note: Recent events (from 1980 on) were additionally picked using events listed on this website: https://www.ggweather.com/enso/oni.htm (Date accessed: 18 October 2018)

Table 6: Overview of all events found in the coral Sr/Ca records and of El Niño and La Niña events of corresponding time periods listed in publications. Events in coral records were matched with published events in consideration of age model uncertainties of each coral record.

Introduction. This file includes supplementary methods, pictures of sampling locations (Fig. S1), X-ray images of the coral samples (Fig. S2), photomicrographs of the coral samples (Figs. S3-S5), power spectrum analysis plots of non-detrended coral SST anomalies (Fig. S6), wavelet power spectra of all coral records (Fig. S7), plots with Sr/Ca-SST anomalies and anomalies after detrending (Fig. S8), singular spectrum analysis (SSA) plots (Figs. S9-S11) and power spectrum analysis plots of detrended coral SST (Fig. S12) including text descriptions. Two additional tables giving the years of El Niño and La Niña events used for the composite maps (Table S1) and the linear regression results between the coral SST records and the Wilson Niño Index (Table S2) are also part of this supplementary material.

1 Supplementary Methods

Indices

We use Niño 3.4 SST anomalies taken from NOAA ERSSTv5 (Huang et al. 2017) for power spectrum analysis (Fig. S12). These have been interpolated from sparse observational data and extend back until 1870.

Statistics

Power spectra analysis was performed twice using the spectral analysis function REDFIT (Welch window) of the open source software *PAST* (version 3.25; Hammer et al., 2001). One run was performed with the time series before detrending, one run after detrending. Every time series was detrended using the softwares *breakfit* (Mudelsee, 2009) or *rampfit* (Mudelsee, 2000), respectively (Fig. S8).

SSA (Vautard and Ghil, 1989) were generated using the *MATLAB* (version R2019b) software toolboxes by Groth and Ghil (2015).

2 Table with years of events that were used in the composite maps (Fig. 2 of the main document)

Event years	
El Niño	La Niña
1982/83	1984/85
1986/87	1988/89
1987/88	1995/95
1991/92	1998/99
1994/95	1999/00
1997/98	2007/08
2002/03	2010/11
2009/10	2011/12
2015/16	

Table S1: El Niño and La Niña event years used for the composite maps. Between 1982 and 2016, 9 El Niño events and 8 La Niña events occurred. Temperature anomalies from December to February were averaged for each event.

3 Pictures of coral sample sites

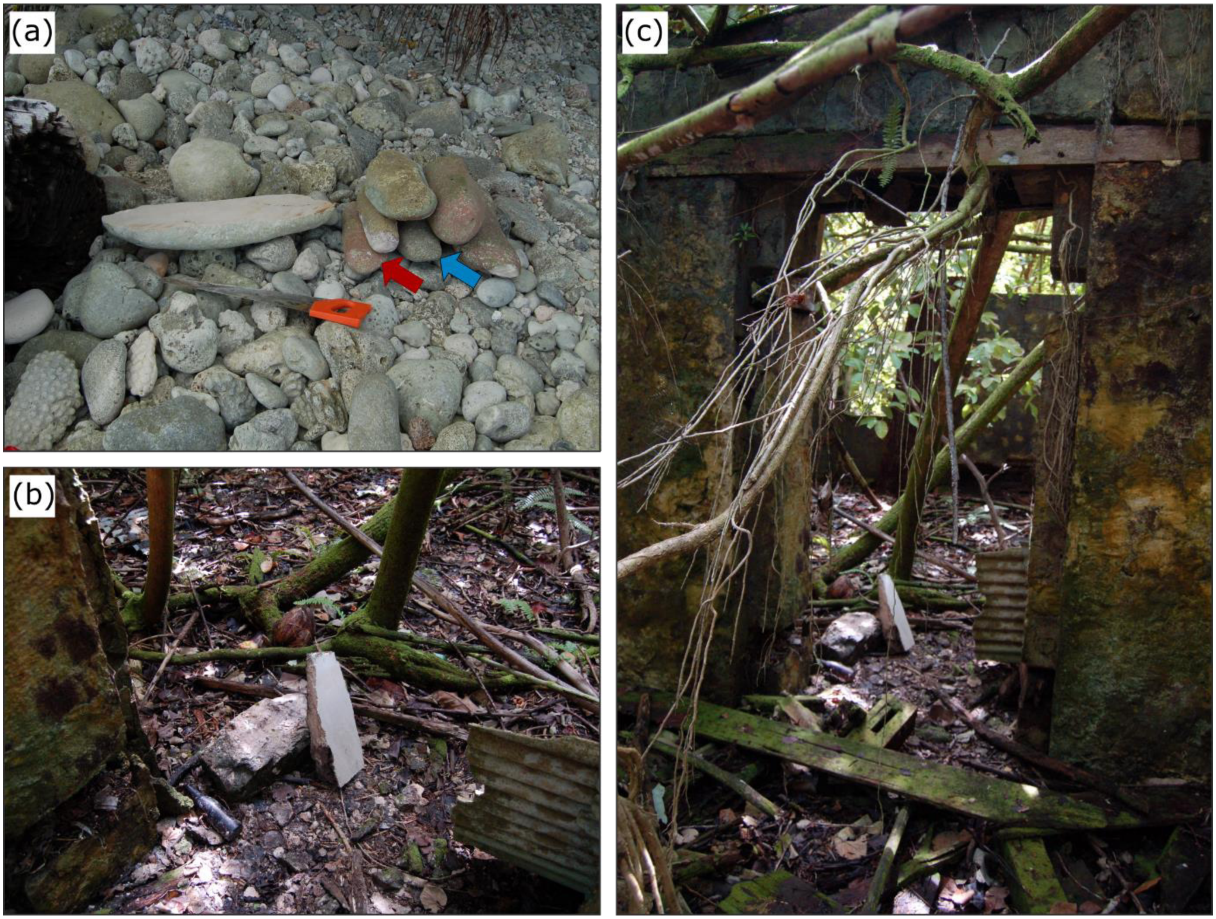

Figure S1: Pictures of coral sample sites. (a) Boulder beach at Eagle Island where the samples E5 (1675-1716; blue arrow) and E3 (1870-1909; red arrow) were collected. (b) and (c) a derelict building at Boddam Island from which the sample B8 (1836-1867) was collected.

4 X-ray images

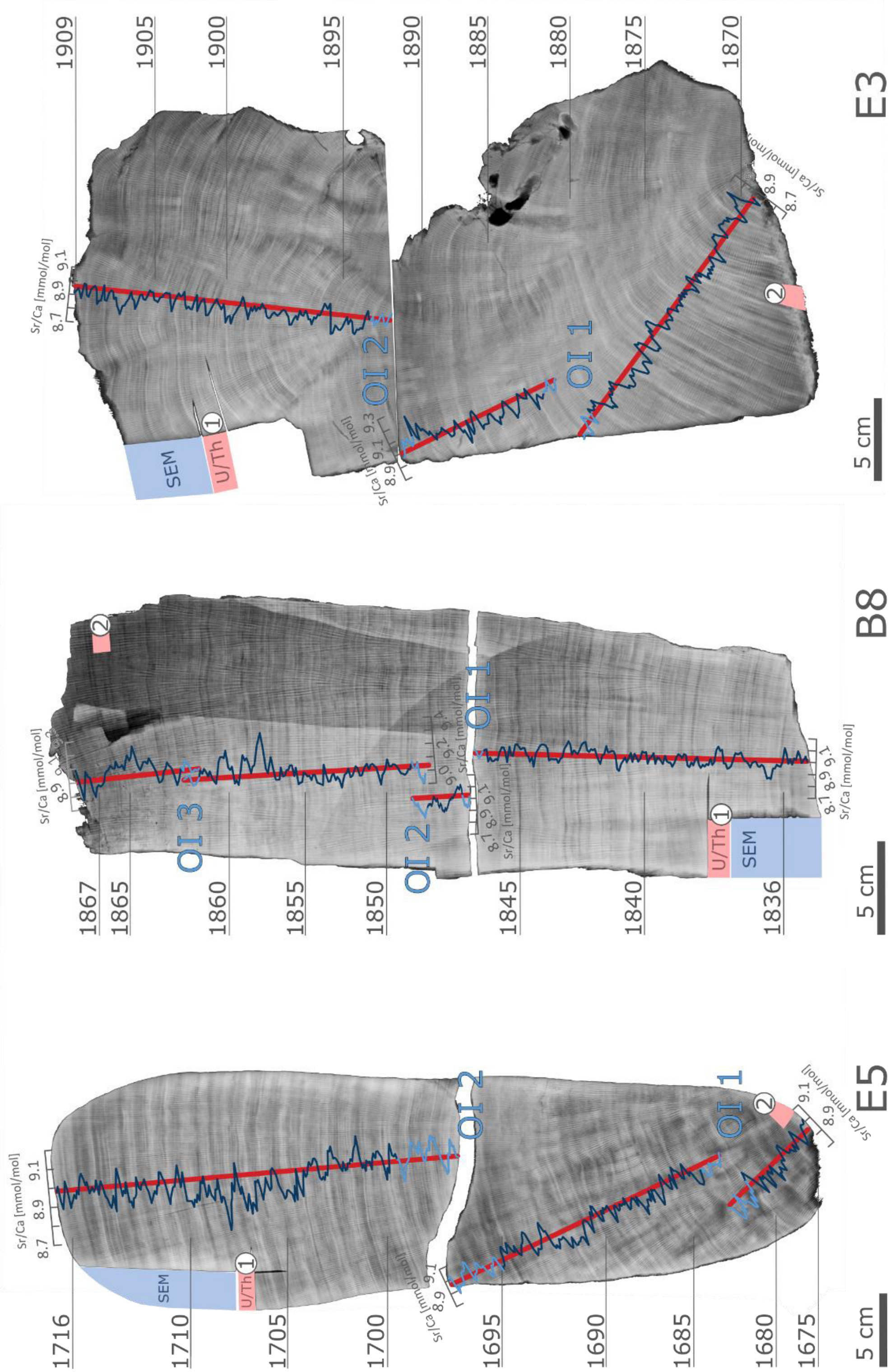

Figure S2: X-ray images of coral samples analyzed in this study with raw Sr/Ca data (dark blue lines with overlapping intervals (OI) in light blue). Age models were interpreted using two U/Th measurements from each sample (sampling points for U/Th dating are indicated with circled numbers and light red-shaded areas; for determined ages see Table 1). Red lines indicate subsampling paths. Blue-shaded areas indicate sampling locations for subsamples used for Scanning Electron Microscopy (SEM). Please note that the slab of sample B8 is uneven as the slab was too brittle to polish out saw cuttings from field work and these are still seen on the X-ray image. Note the even growth patterns of all samples.

5 Thin section and SEM analysis images

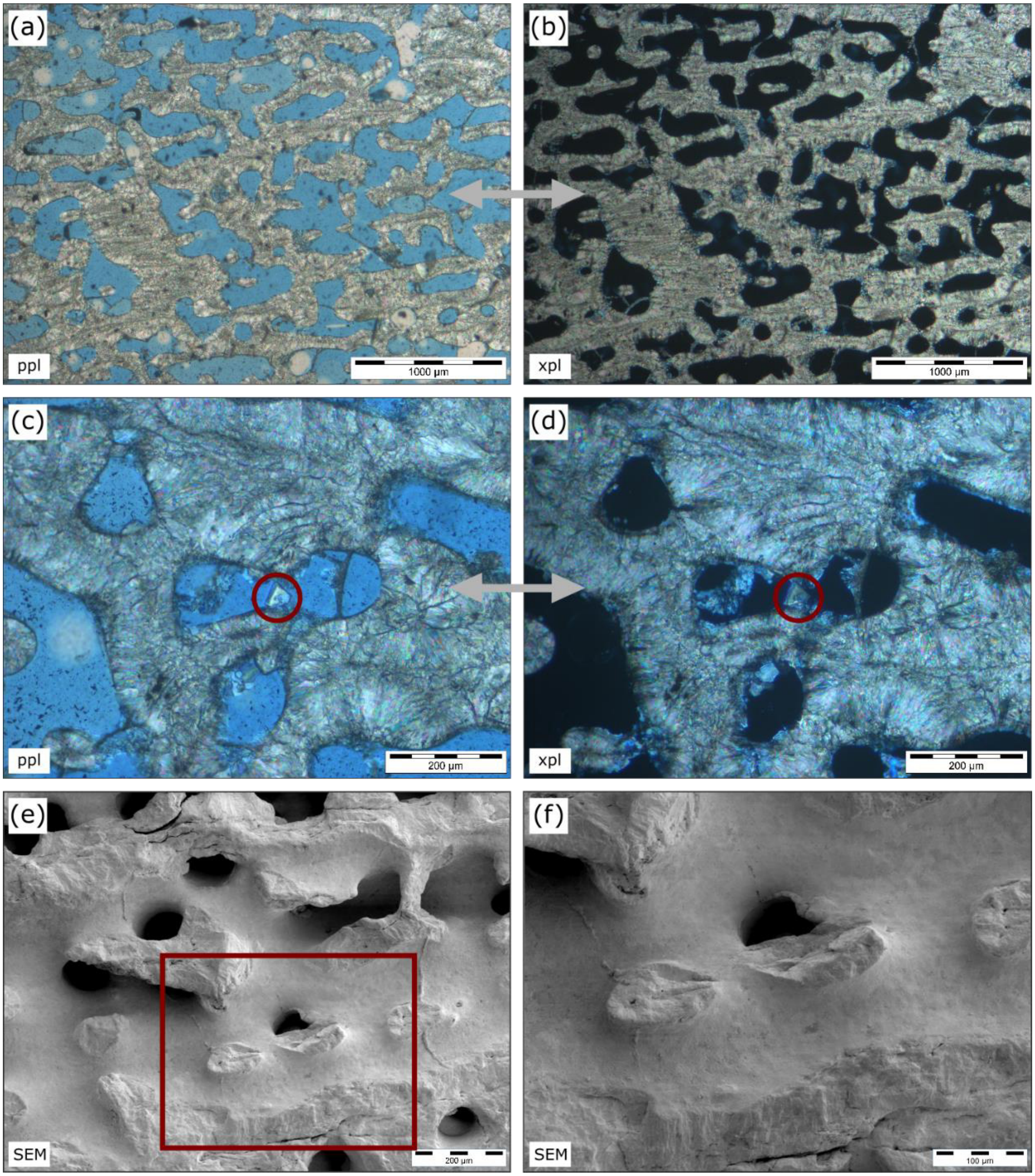

Figure S3: Photomicrographs of coral sample E5 (1675-1716). Double arrows indicate corresponding photomicrographs. (a) PPL and (b) XPL overview photomicrograph of the coral skeleton. (c) PPL and (d) XPL photomicrograph of the sample at higher resolution where minor amounts of secondary calcite cement are visible (red circle). (e) SEM overview and (f) detail image (red box in e) where only trace amounts of sugary cements can be found.

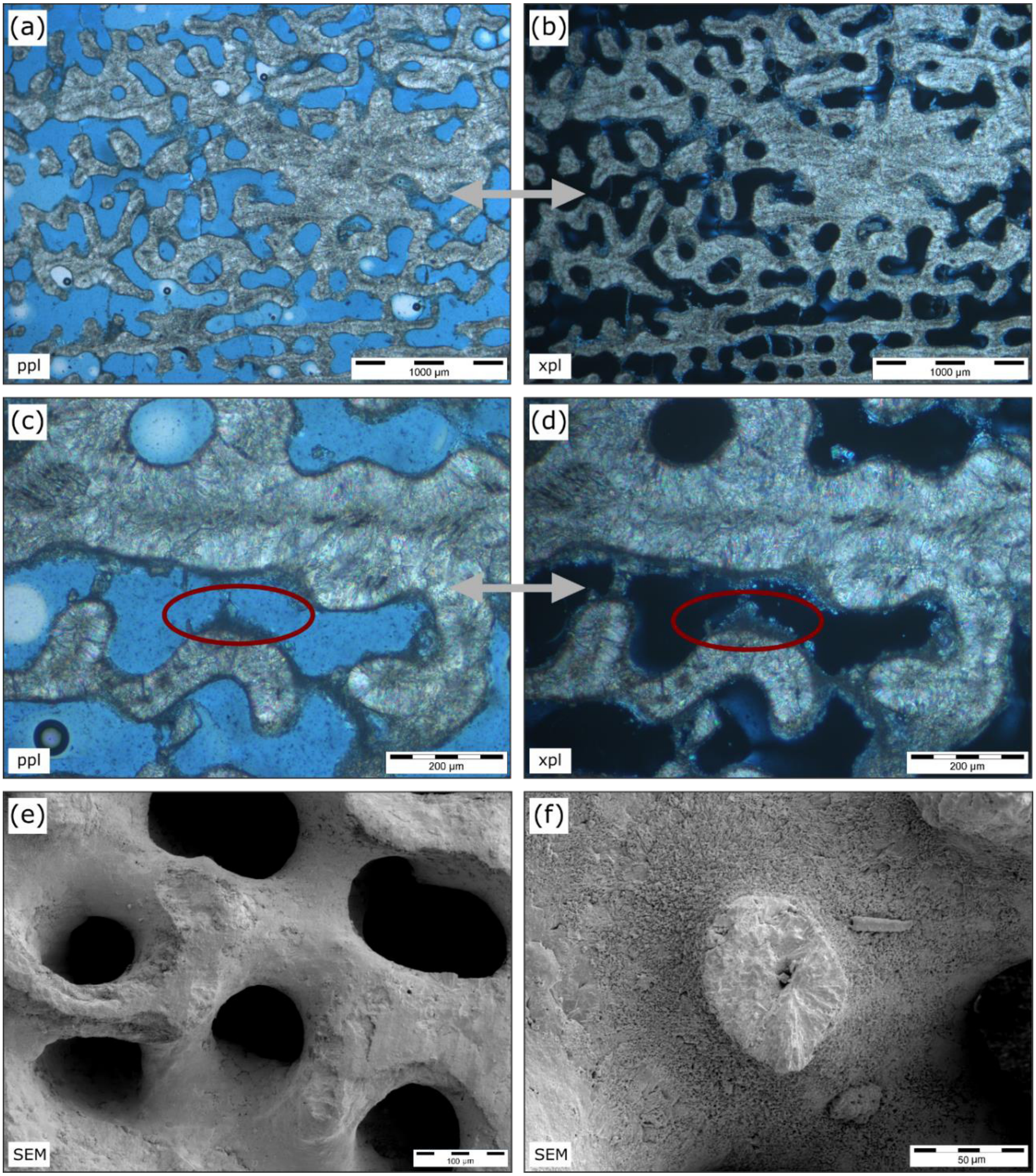

Figure S4: Photomicrographs of coral sample B8 (1836-1867). Double arrows indicate corresponding photomicrographs. (a) PPL and (b) XPL overview photomicrograph of the coral skeleton. (c) PPL and (d) XPL photomicrograph of the sample at higher resolution where small amounts of secondary aragonite cement are visible (red oval). (e) SEM overview and (f) detail image of B8 (1836-1867). Small amounts of sugary aragonitic cement can be seen.

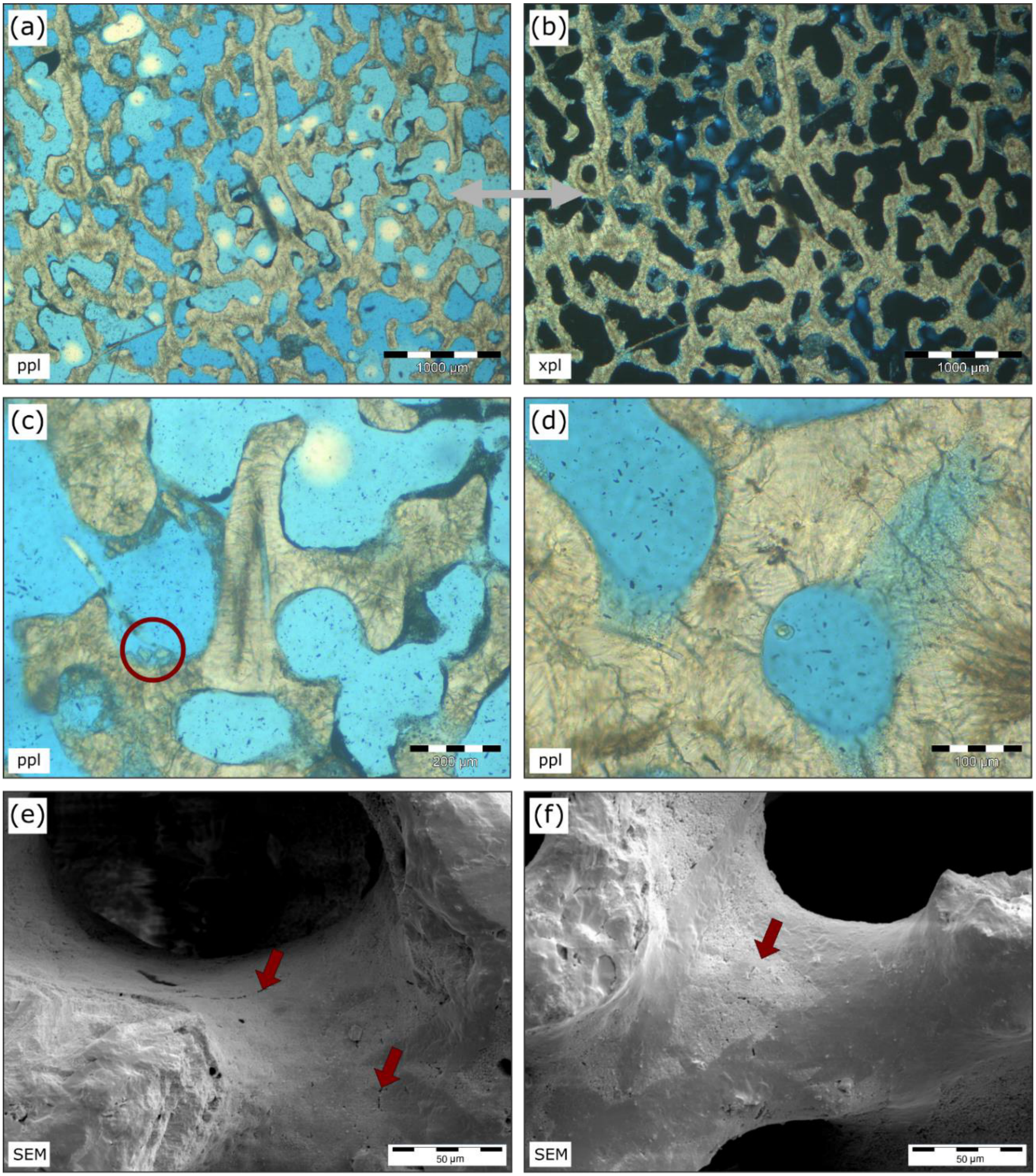

Figure S5: Photomicrographs of coral sample E3 (1870-1909). Double arrows indicate corresponding photomicrographs. (a) PPL and (b) XPL overview photomicrograph of the coral skeleton. (c) PPL photomicrograph of the sample at higher resolution where small fragments of aragonite are found (red circle). (d) PPL microphotograph of the sample at higher resolution without any signs of diagenesis. SEM images showing (e) microborings (red arrows) and (f) areas which appear brighter due to dissolution.

6 Seasonal cycles inferred from Singular Spectrum Analysis

Singular spectrum analysis (SSA) of the coral records with seasonal cycles reveal large interannual to decadal SST variabilities during both the 17-18th century and 19-20th century (not shown). The reconstructed components 2 and 3 (RC2, RC3) produced by SSA describe seasonal amplitudes for all samples and explain 28% (E5), 26% (B8), 32% (E3) of the coral Sr/Ca-SST variance. Decadal variabilities are larger during the 17-18th century compared to the 19-20th century. The first reconstructed component (RC1) of E5 with seasonal cycles explains 48% of the coral Sr/Ca-SST variance and describes a periodicity of around 18 years. The coral records covering the 19-20th century do not show a strong decadal component in SSA. Instead, RC1 explains 49% (B8) and 39% (E3) of the coral Sr/Ca-SST variance and describes a periodicity of around 7 years, which can be interpreted as ENSO periodicity.

The SSA results were validated by power spectrum analysis of bimonthly resolved coral SST anomalies, which were not detrended (Fig. S6). For this analysis, the coral record GIM (Pfeiffer et al., 2017) was included, which extends from 1880 to 1995. Power spectrum analysis of E5 (Fig. S6a) shows a low-frequency band corresponding to a periodicity of 18-19 years, identical to RC1 of the SSA. In addition, RC2 describing an ENSO periodicity of 4-5 years is confirmed by the second highest low-frequency band in power spectrum analysis of E5. The power spectrum analysis of the corals covering the 19-20th century (B8 and E3) confirms their SSA results, as well (Figs. S6b & c). It shows high power on the low-frequency (5-6 years for B8; 6-7 years for E3) band, which was also described by the first reconstructed components in SSA. Power spectrum analysis for GIM (Fig. S6d) reveals high power on the ENSO band (4-5 years and 8 years) and the highest power at the decadal frequencies (26 years).

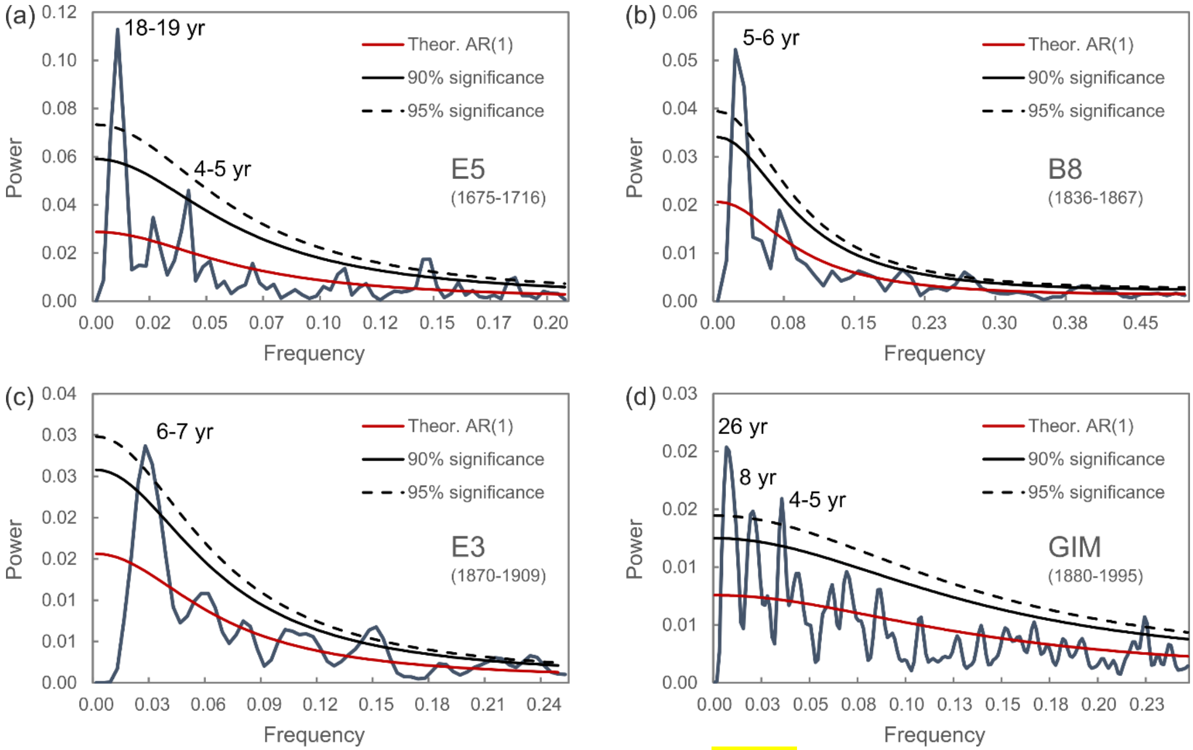

Figure S6: Power spectrum analysis of each Chagos coral bimonthly resolved anomaly series.

7 Wavelet Power Spectra

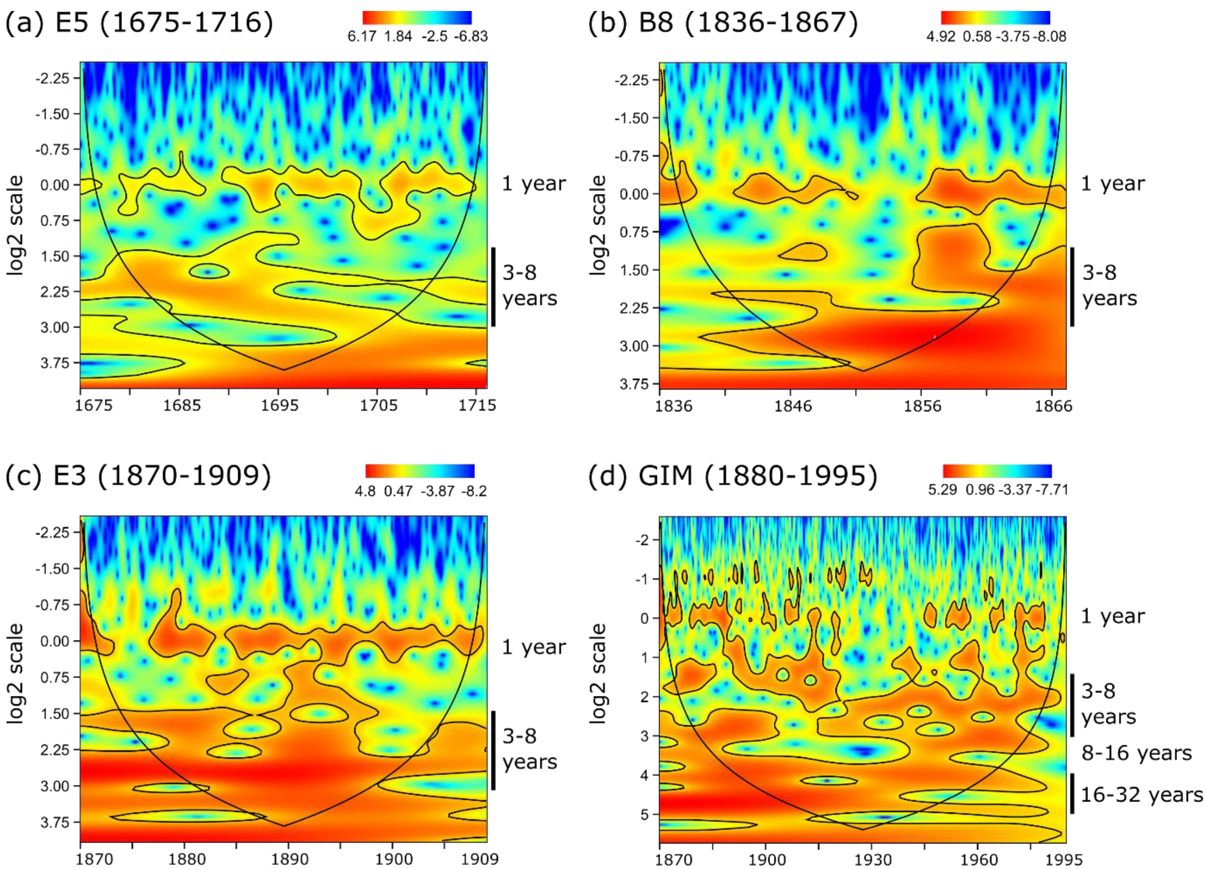

Figure S7: Wavelet power spectra of (a) E5 (1675-1716), (b) B8 (1836-1867), (c) E3 (1870-1909) and (d) GIM (1880-1995) coral Sr/Ca records. Wavelet power spectra were computed using the Morlet wavelet. The cone of influence and the 95% confidence level are indicated by the black lines. All spectra were computed with the free software package PAST (version 3.25; Hammer et al., 2001).

8 Detrending of coral SST records

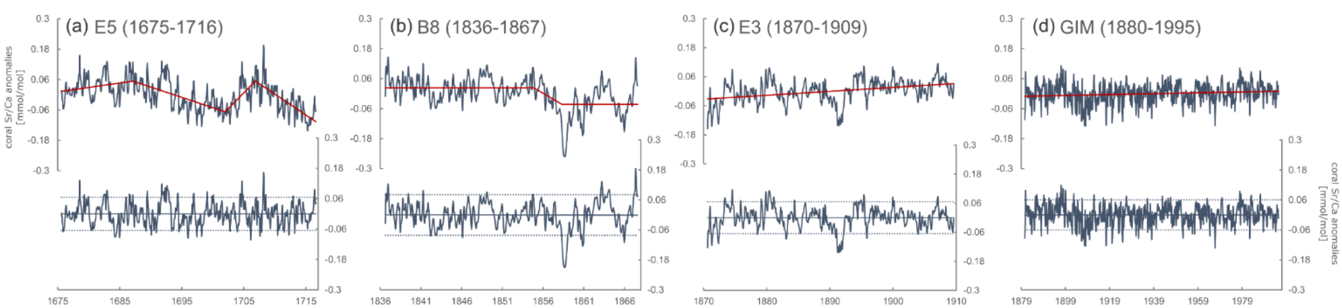

Figure S8: Sr/Ca-SST anomalies with calculated trend lines (red lines; upper plot) and anomalies after detrending (lower plot; with plotted 1.5x of the standard deviation as dashed lines) for the coral records (a) E5 (1675-1716), (b) B8 (1836-1867), (c) E3 (1870-1909) and (d) GIM (1880-1995).

9 Interannual SST variability inferred from Singular Spectrum Analysis

The spectral results of the coral records with seasonal cycles were validated by singular spectrum analysis (SSA) of coral SST anomalies records and power spectrum analysis, to reveal stronger patterns of variance when seasonal cycles were subtracted (Figs. S9-S12). During the 17-18th century, the coral record shows a periodicity of 18 years in RC1, which explains 47% of the coral Sr/Ca-SST variance (Fig. S9). The second reconstructed component (RC2; Fig. S9) of E5 (1675-1716) explains 14% of the coral Sr/Ca-SST variance and describes an ENSO periodicity of 4-5 years. During the 19-20th century, the pattern of variance describing the ENSO periodicity in the coral records are found in two to three reconstructed components: For B8 (1836-1867), RC2 and RC3 describe an ENSO periodicity of 5-8 years with in total 62% of the corals Sr/Ca-SST variability (Fig. S10). For E3 (1870-1909) it is even higher with RC1-3 explaining 65% of the coral Sr/Ca-SST variance. Those three components describe a characteristic ENSO periodicity of 3-8 years (Fig. S11).

Power spectra of detrended coral SST time series all show the typical ENSO periodicity between 3 and 8 years (Fig. S12a-d). Those periodicities can also be found in the power spectra of the Niño3.4 indices (Fig. S12e & f). Even after detrending, the power spectrum of the GIM coral SST record still shows the highest power at low-frequencies, which translates to a period of 21-22 years.

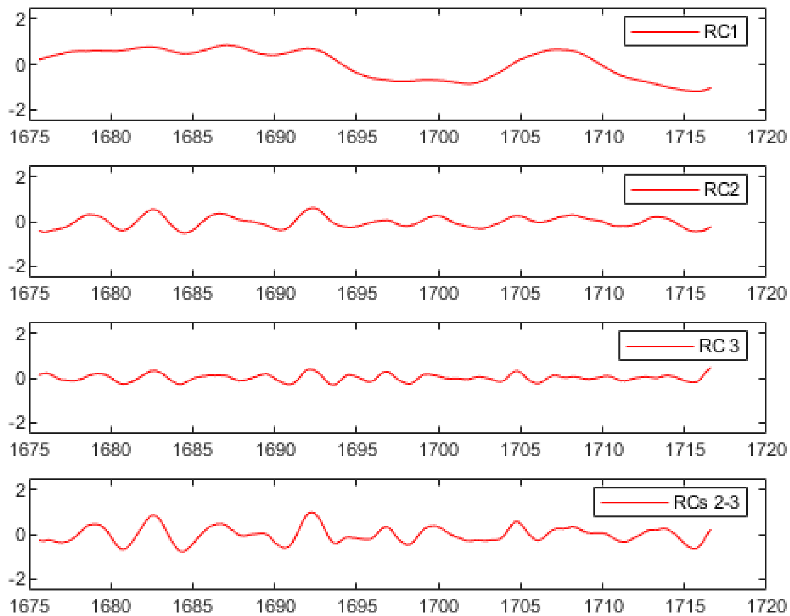

Figure S9: Reconstructed components from Singular Spectrum Analysis of E5 (1675-1716) Sr/Ca monthly anomalies. First reconstructed component (RC1) describes a periodicity of 18 years. RC2 and RC3 describe typical ENSO periodicities.

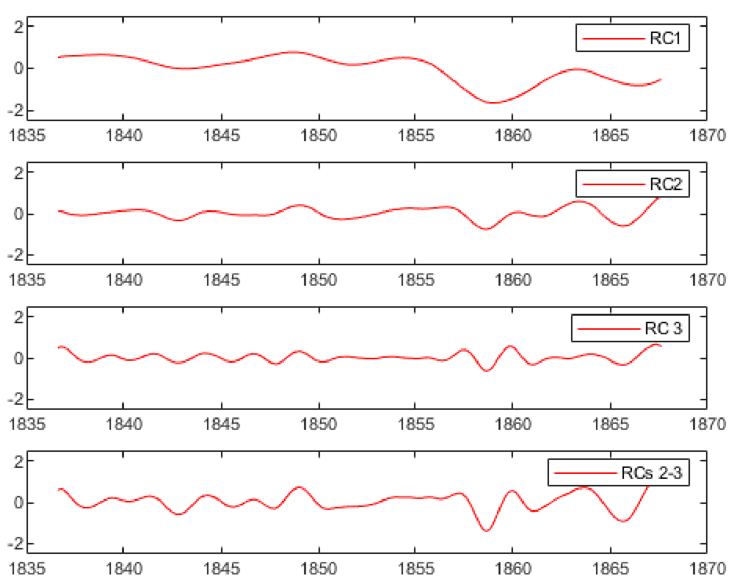

Figure S10: As Figure S9, but for coral Sr/Ca record of B8 (1836-1867).

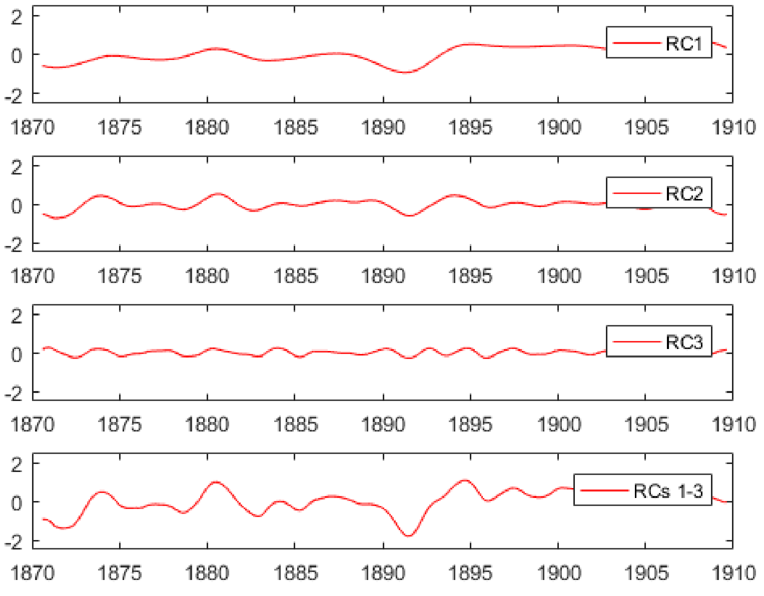

Figure S11: As Figures S9 and S10, but for coral Sr/Ca record of E3 (1870-1909). ENSO periodicities are described by all shown reconstructed components RC1-3.

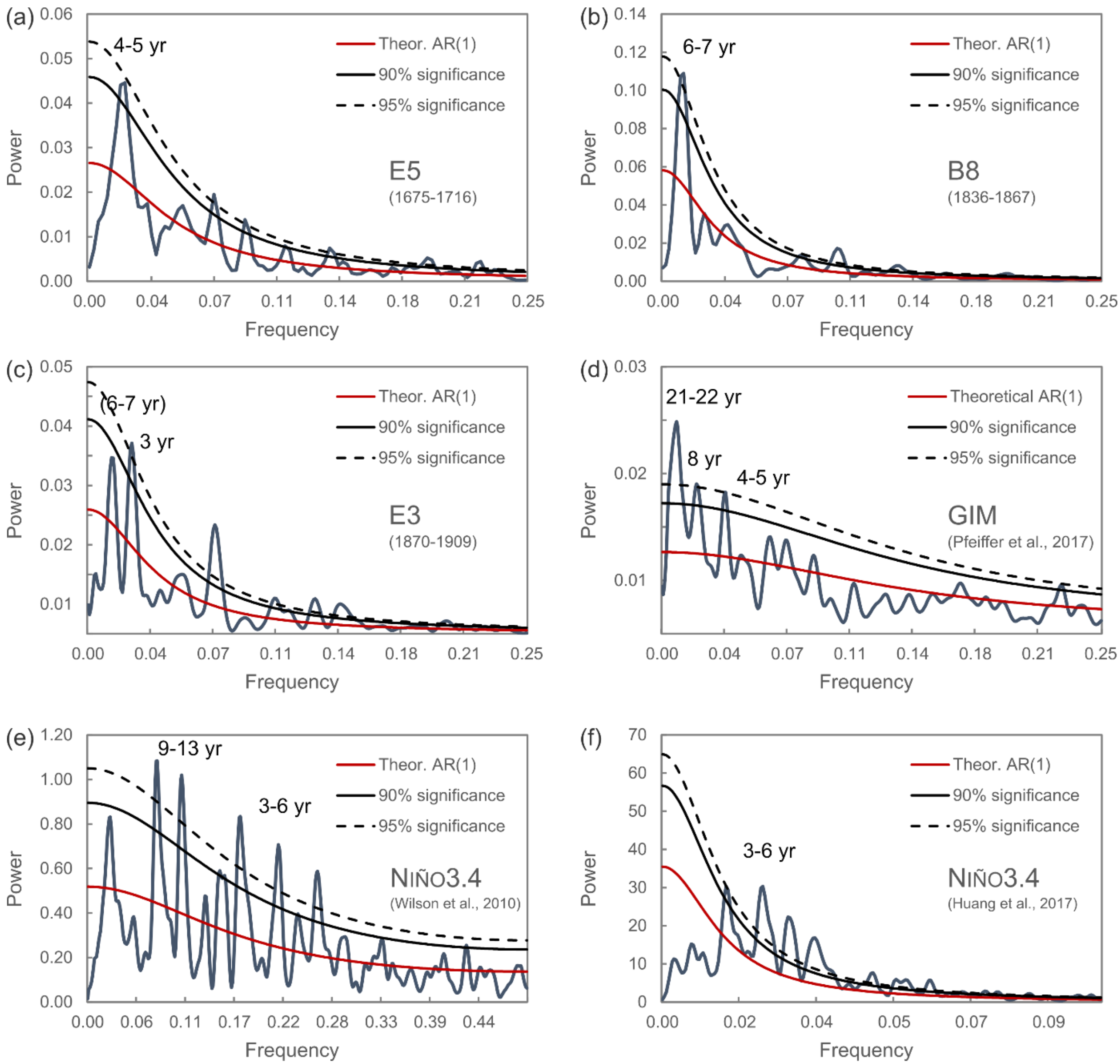

Figure S12: Power spectrum analysis plots for detrended coral SST, the annually resolved Wilson Niño index (Wilson et al., 2010) and the monthly resolved Niño3.4 index based on NOAA ERSSTv5 (Huang et al., 2017) time series.

10 Linear regression

Ordinary least square (OLS) regression and *PearsonT3* calculation results reveal no significant linear relation between annual coral SST records and the Wilson Niño index (Table S2).

Method	Coefficient	E5 (1675-1716)	B8 (1836-1867)	E3 (1870-1909)	GIM (1880-1995)
Excel OLS	R^2 (p-value)	4.09E-5 (0.9679)	0.0006 (0.8979)	0.0027 (0.7502)	0.0444 (0.0232)
PearsonT3	r [95% confidence interval]	-0.006 [-0.361; 0.350]	-0.024 [-0.739; 0.716]	0.052 [-0.418; 0.500]	0.211 [-0.005; 0.408]

Table S2: Correlation coefficients of given coral records with the Wilson Niño index.

Supplementary References

Groth, A., and Ghil, M.: Monte Carlo Singular Spectrum Analysis (SSA) revisited: Detecting oscillator clusters in multivariate datasets, J. Climate, 28, 7873-7893, https://doi.org/10.1175/JCLI-D-15-0100.1, 2015.

Hammer, Ø., Harper, D. A. T., and Ryan, P. D.: Paleontological statistics software: package for education and data analysis, Palaeontol. Electron., (4), 2001.

Huang, B., Thorne, P. W., Banzon, V. F., Boyer, T., Chepurin, G., Lawrimore, J. H., ... and Zhang, H. M.: Extended reconstructed sea surface temperature, version 5 (ERSSTv5): upgrades, validations, and intercomparisons, J. Climate, 30(20), 8179-8205, https://doi.org/10.1175/jcli-d-16-0836.1, 2017.

Mudelsee, M.: Ramp function regression: A tool for quantifying climate transitions, Comput. Geosci.-UK, 26(3), 293-307, https://doi.org/10.1016/s0098-3004(99)00141-7, 2000.

Mudelsee, M.: Break function regression: A tool for quantifying trend changes in climate time series, Eur. Phys. J.-Spec. Top., 174(1), 49-63, https://doi.org/10.1140/epjst/e2009-01089-3, 2009.

Pfeiffer, M., Zinke, J., Dullo, W. C., Garbe-Schönberg, D., Latif, M., and Weber, M. E.: Indian Ocean corals reveal crucial role of World War II bias for twentieth century warming estimates, Sci. Rep.-UK, 7(1), 14434, https://doi.org/10.1038/s41598-017-14352-6, 2017.

Vautard, R., and Ghil, M.: Singular spectrum analysis in nonlinear dynamics, with applications to paleoclimatic time series, Physica D, 35, 395-424, https://doi.org/10.1016/0167-2789(89)90077-8, 1989.

Wilson, R., Cook, E., D'Arrigo, R., Riedwyl, N., Evans, M. N., Tudhope, A., and Allan, R.: Reconstructing ENSO: the influence of method, proxy data, climate forcing and teleconnections, J. Quaternary Sci., 25(1), 62-78, https://doi.org/10.1002/jqs.1297, 2010.